Journal of Energy Storage 84 (2024) 110964

Contents lists available at ScienceDirect

Journal of Energy Storage

journal homepage: www.elsevier.com/locate/est

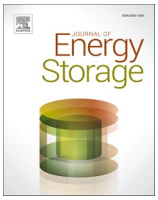

Research papers

Innovative power smoothing techniques for wind turbines using batteries and adaptive pitch regulation

Claudio Galli, Francesco Superchi, Francesco Papi, Giovanni Ferrara, Alessandro Bianchini *

Department of Industrial Engineering, Università degli Studi di Firenze, Via di Santa Marta 3, 50139 Firenze, Italy

ARTICLE INFO

Keywords:
Wind turbine
Power smoothing
Pitch control
Battery

ABSTRACT

To ensure a higher penetration of wind energy in local and national energy mixes, power variability induced by wind fluctuations needs to be limited. In this study, three power smoothing approaches are proposed and compared to the conventional unconstrained behavior. The first method makes use only of a state-of-the-art Li-Ion battery (BESS), while the second and the third also integrate a dedicated blade pitch regulation to control the power output; more specifically, in one case pitch regulation is used to curtail ramp-up violation, i.e. an abrupt increase in wind speed and power output that exceeds an imposed maximum variation threshold, if the BESS cannot be charged completely. In the third method, pitch actuators are exploited to contrast ramp-down violations in addition to ramp-up violations, by reducing the amount of power fed to the grid for specific wind speeds. The three methods have been applied to a hypothetical case study including the NREL 5 MW Reference wind turbine subject to a series of 20-year wind data synthesized based on experimental data coming from a wind farm in Greece. A power ramp rate limit equal to 10 % of the nominal power per minute has been considered, and the economic prospects of the system have been studied from the perspective of different penalties (0–500 €/MWh of violating energy) that could be applied in the future to ramp rate violations. Results obtained show that: i) below a 20 €/MWh penalty, it is not convenient to add any power smoothing method; ii) for a 20–60 €/MWh penalty, it is convenient to add a battery only; iii) for a 60–350 €/MWh penalty adding a pitch control system to the BESS to avoid ramp up violations if the battery is fully charged becomes convenient; iv) above 350 €/MWh, the best control method is a hybrid battery and pitch system which modifies the power curve of the turbine to obtain an optimal compromise between power smoothing and power production reduction. Focusing, however, on the quality improvement of wind turbine power output, abatement ratios for proposed innovative methods range from around 84 % to 88 %, and the average intensity of those violations is reduced to around 17–19 % compared to a standard operation. All these metrics are much higher than those achievable with the use of a battery alone.

1. Introduction

Consensus is established about the fact that wind energy represents one of the backbones of the future energy mix worldwide, thanks to its industrial maturity and competitive Levelized Cost of Energy among renewables [1]. One of the main issues that prevent a wider distribution of wind energy is related to the fluctuating nature of wind resources, which may lead to stability issues for the grid [2] such as, for example, changes in grid frequency, variations of active and reactive power, and voltage flicker (e.g., see [3,4]). Therefore, to boost wind energy penetration, enhancements of output power quality are foreseen in the near future, via techniques such as power smoothing [5]. The goal is to set a limit on the allowed amount of increase or decrease of power within a defined timescale (e.g., 1 min). This is usually achieved by some sort of storage system.

The state of the art regarding power smoothing techniques offers many different approaches to the problem. The simplest method consists of integrating a traditional BESS in an energy production system to mitigate power fluctuations. Authors in [5] proved the effectiveness of Li-Ion batteries when introduced in a combined solar PV-Wind farm microgrid in Hawaii. Another successful implementation of a BESS for power smoothing was reported in [6], where a 20-year techno-economic analysis implementing ramp rates was carried out for a single 2 MW turbine. Authors in [7] highlighted the importance and effectiveness of a hybrid MPPT BESS power management strategy when integrated

* Corresponding author.
E-mail address: alessandro.bianchini@unifi.it (A. Bianchini).

https://doi.org/10.1016/j.est.2024.110964
Received 5 September 2023; Received in revised form 12 January 2024; Accepted 12 February 2024
Available online 20 February 2024

Nomenclature

CP	Power Coefficient
TSR	Tip Speed Ratio
HAWT	Horizontal Axis Wind Turbine
WT	Wind Turbine
LCoE	Levelized Cost of Energy
RR	Ramp Rate
RRV	Ramp Rate Violation
RDV	Ramp-down Violation
RUV	Ramp-up Violation
NREL	National Renewable Energy Laboratory
DE	Differential Evolution
NPV	Net Present Value
SoC	State of Charge
SoH	State of Health
UCL	Upper Charge Limit
LDL	Lower Discharge Limit
ODL	Optimal Discharge Limit
OCL	Optimal Charge Limit
WS	Wind Speed
WS_{MAX}	Maximum Wind Speed
WS_{MIN}	Minimum Wind Speed
WS_{MEAN}	Mean Wind Speed
BESS	Battery Energy Storage System
HESS	Hybrid Energy Storage System
FESS	Flywheel Energy Storage System
DES	Double Exponential Smoothing
SES	Single Exponential Smoothing
PI	Proportional Integral
BPA	Bonneville Power Administration
DoD	Depth of Discharge
O&M	Operations & Maintenance
CAPEX	Capital Expenditures
BAT	Battery
PA+	Pitch Assisted UP
PA∓	Pitch Assisted UP/DOWN
C_{RATE}	Charge rate
MPPT	Maximum Power Point Tracking
MPC	Model Predictive Control

together with a small wind turbine. Further developments have also been made on the BESS system: the integration in a wind park of a Li-Ion battery with a discrete wavelet transform method has proven to enhance smoothing capabilities and slow its degradation [8]. Moreover, authors in [9] provided valuable information when reviewing the different BESS control techniques, mainly divided into PI, Fuzzy, and MPC strategies.

As discussed in [3], BESS appears to be the most effective smoothing storage system assuming that an intelligent control logic is applied. However, other devices have been investigated with some degree of effectiveness, such as flywheels. In some grids, they are used for power smoothing due to their high and fast power supply [10]. Authors in [11] confronted FESS and BESS for power smoothing of a 200 kW wind turbine: flywheels proved to be an economic and viable storage system with up to 80 % ramp rates abatement ratios. Supercapacitors have also been integrated into wind farms to mitigate voltage flicker [12]. In [13], a HESS consisting of a supercapacitor and an electrochemical battery applied to solar PV production improved the power quality of the system while reducing the stress on the BESS. Overall, when compared to more traditional electrochemical batteries (such as Li-Ion), these devices showed great power quality boosts but provided a much smaller energy reserve for equal investment cost [14]. Other forms of mechanical energy storage, such as pumped hydro plants or compressed air storage have been investigated in [15], highlighting their effectiveness, limited however by their spatial or geographical constraints. The integration of a storage system has been shown, however, to significantly impact the economy of the system [3].

To this end, studies have been made to understand if innovative control techniques can be alternatively used or coupled with BESS to enhance power quality at a lower cost. For this reason, the implementation of fuzzy control logic for pitch actuators to smooth the power output of the turbine is widely studied in the literature [16]. In [4], two methods of smoothing were studied with a double controller based on an exponential moving average, granting power reductions as low as 4.7 % and 8.28 %. Similar results were observed in [17], where DES and SES fuzzy control logics were confronted in periodic shaped wind data. Authors in [18] also reported an improved smoothing power profile when implementing a hybrid Fuzzy-PI controller. Such a technique provides power quality increase, without the huge investment cost of storage devices. These studies served as a baseline to prove how a more dynamic use of pitch actuators could smooth power fluctuations. However, none of those works reports a techno-economic analysis of the system, studying the economic loss coming from curtailed power production in actual plant integration.

The rationale of the present study moves from the consideration that modern wind turbines feature quite advanced regulation strategies based on blade pitch control. These mechanisms are very well-known, accurate, and reliable. The idea is therefore to investigate if adding pitch control as an additional degree of freedom to the power smoothing logic can have a positive impact on the cost-competitiveness and effectiveness of such logic, especially if future scenarios are foreseen, in which energy outputs violating the grid ramp limits are penalized or even prohibited. For the first innovative method proposed, pitch control is activated when the storage is completely or almost full, or when the charge rate limit is reached, ensuring that no ramp-up violations are allowed. This simple strategy allows to effectively contrast ramp-up violations but does not help in case of ramp-down events – i.e., rapid decreases in power output. To overcome this limitation, additional features were introduced, allowing pitch control to also contrast ramp-down violations. This additional method is based on the idea of reducing the power curve of the wind turbine in selected wind speed ranges to charge the storage system (or with the aid of the already mentioned additional pitch system), while at the same time achieving a smoother power fed into the grid. To evaluate the potential of these techniques, the improved stability of the system is valued through the introduction of economic penalties calculated on the amount of energy that violates the ramp-rate limit. The introduction of power-quality requirements for renewable energy generation systems is a topic of active debate within the scientific community, as grid regulation rules are decided by local operators. Various grid operators have applied penalties to promote higher quality wind power produced. Some of those penalties are fixed and dependent strictly on the wind capacity installed (i.e., BPA [19]), while others are calculated as fractions of up and down-regulation prices ([20,21]). In more extreme cases, such as China for example, the large capacity of wind power installed, combined with an unstable grid, has been subject to huge amounts of wind power curtailments and energy waste done by either shutting down the turbine or reducing its power output [22]. Given the lack of consensus, a sensitivity analysis is conducted in this work, incorporating a range of economic penalties to offer guidance for future scenarios.

The study is structured as follows. Section 2 reports in detail the specific case study analyzed, starting from the wind power generation system and going over the BESS specific application and control. In Section 3, the technical grid parameters of power quality and ramp rate limit are introduced, together with the economic penalties applied for

limit violations. The crucial part of this work is then reported in Section 4, where the three different power smoothing methods proposed are explained in detail before focusing on the economic optimization of the plant net present value. Then, techno-economic results regarding the system retribution and power quality are highlighted in Section 5, together with the optimization parameters of the various scenarios analyzed. Lastly, the objectives and outcomings of this paper are summed up in the conclusions in Section 6.

2. Case study

2.1. Wind turbine and resource data

The turbine model used to demonstrate the proposed power smoothing techniques is the well-known NREL reference 5 MW turbine, an open turbine concept that is representative of state-of-the-art multi-megawatt turbines with variable speed and variable blade-pitch-to-feather-control. The turbine model was built using data from [23], where detailed information about the power curve, tip speed ratio, rotor speed, pitch angle and other parameters necessary for the wind power calculations are given (Fig. 1).

2.1.1. Wind data

Wind data history harvested in the onshore wind farm of Kedros, Greece, was used. Wind speed values were measured by an anemometer at hub height mounted on a 2.3 MW turbine (ENERCON E-82) and recorded with a ten-minute resolution for five years. This dataset provided the maximum, minimum and mean wind speed values (WS_{MAX}, WS_{MIN}, WS_{MEAN} respectively). This data set has been already analyzed and successfully used for energy-production estimates in [8].

2.1.2. Post-processing of wind time series

To properly evaluate the ramp rates and study the power variation minute by minute, an increase in the temporal resolution of the original data was needed. An iterative procedure was followed with the aid of a Python script to reach a finer dataset. The function generates ten WS values that maintain the same average as WS_{MEAN}. To fill the missing information, eight random values between WS_{MAX} and WS_{MIN} are iteratively generated until the 10-minute average WS_{MEAN} is respected. In other words, WS_{MEAN} was multiplied by nine and was subtracted from it the sum of eight values of wind speed randomly generated (between WS_{MIN} and WS_{MAX}) to obtain a residual as of Eq. (1). This residual was accepted if higher than WS_{MIN} and lower than WS_{MAX}.

$$RESIDUAL = 9 \cdot WS_{MEAN} - \sum_{i=1}^{8} WS_{i,RNDM} \quad (1)$$

where $WS_{i,\ RNDM}$ refers to the i^{th} element of wind speed randomly generated. This was done using a Python function, which generates 8 random numbers in the range of WS_{MIN} and WS_{MAX}.

The ten values of wind speeds are then composed of the eight random WS values together with the residual and WS_{MEAN}, obtaining a one-minute time step data frame for five years of operation. This procedure has been proven in [8] to provide data sets that can be considered representative of natural wind fluctuations expected in the site. The next 15 years are composed of randomly-selected corresponding months of the first five years. The following analyses were based on a 20-year wind speed dataset with 1-minute resolution.

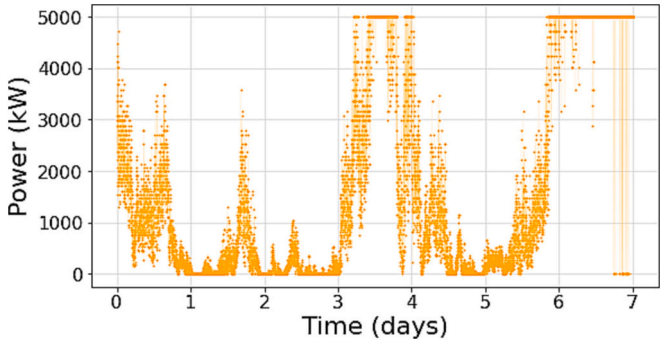

Fig. 1. Power produced minute by minute by the turbine, sample of February 2015.

2.1.3. Power calculations

Attended power production is obtained in a conventional way based on Eq. (2):

$$P_{EL} = \frac{1}{2}\eta_{EL}\rho A C_P V^3 \quad (2)$$

where:

- P_{EL} is the electric power fed to the grid in kW
- V is the one-minute mean wind speed at the rotor hub in m/s
- C_P is the turbine power coefficient, derived from the turbine datasheet
- ρ is the nominal air density, corresponding to 1.225 kg/m^3
- A is the area swept by the rotor, equal to 12,445.3 m^2 for the turbine under consideration
- η_{EL} is the electric efficiency of conversion from mechanical to electric energy fed into the grid, assumed constant and equal to 0.94 [23]

2.2. Storage system

The presence of a storage system is key for the implementation of a power smoothing system. The technical choices made herein are discussed in the following.

2.2.1. Storage parameters and type

Lithium-Ion batteries were considered in this study due to various reasons. They probably represent the most mature storage technology and among the best ones in the specific energy per unit weight [24]. On the other hand, it is known that cost optimization of Li-ion batteries for large applications is key to ensuring the success of an installation [8]. This kind of optimization will represent one of the tasks of the present study.

2.2.2. Battery degradation

To assess the suitability of the hypothesized battery's use in the new power smoothing strategies, properly accounting for battery degradation is crucial. A battery degradation model was used in this study to assess if batteries need replacement. In particular, according to previous research [8] and based on industrial inputs, the End of Life of the battery is set when one of these two criteria is met; i) in correspondence with a State of Health (SoH) of 70 % ii) after 10 years, even if the State of Health of the battery is above 70 %. The 10-year limit is set based on reliability and safety concerns, and is, to the authors' best knowledge, common industrial practice. The damage of the battery for a regular and constant value of the Depth of Discharge (DoD) is usually calculated via a Wöhler curve obtained through exponential approximation [25,26]. In real operating conditions, however, a battery undergoes charge-discharge cycles of variable amplitudes. To manage this unregular SoC profile, in the present study a Rainflow Counting algorithm developed in [8] has been used to identify the equivalent number of full or half cycles performed by the device [27].

2.2.3. Safeguard criteria

To guarantee a more efficient use of the battery system and contain its degradation over time, additional criteria were introduced. According to the NREL battery degradation model, which has been validated

against experimental data [28], the lifetime of the Li-ion battery that spends most of its time in a SoC between 30 and 50 % is longer than those that spend it in a SoC between 70 and 90 % or 20–40 % [29]. Therefore, additional parameters will be defined.

- Upper Charge Limit of SoC (UCL) - 80 %
- Optimal Charge Limit of SoC (OCL) - 60 %
- Optimal Discharge Limit of SoC (ODL) - 40 %
- Lower Discharge Limit of SoC (LDL) - 20 %

Based on these thresholds, the SoC will never be allowed to go above UCL or below LDL. The battery will be partially charged, instead of fully charged, when its SoC is between OCL and UCL; and partially discharged, instead of fully discharged, when its SoC is between LDL and ODL. According to [30], the procedure can make use of a reference coefficient X described as follows:

Region 1:

$$X_{DISCH} = 1 \; for \; SoC \leq 20\% \tag{3}$$

Region 2:

$$X_{DISCH} = \frac{0.5 - SoC}{0.5} \; for \; 20\% < SoC \leq 40\% \tag{4}$$

Region 3, 4, 5:

$$X_{DISCH} = 0 \; for \; SoC > 40\% \tag{5}$$

Region 1, 2, 3:

$$X_{CHARG} = 0 \; for \; SoC < 60\% \tag{6}$$

Region 4:

$$X_{CHARG} = \frac{SoC - 0.5}{0.5} \; for \; 60\% \leq SoC < 80\% \tag{7}$$

Region 5:

$$X_{CHARG} = 1 \; for \; SoC \geq 80\% \tag{8}$$

X_{DISCH} and X_{CHARG} are both non-dimensional parameters related to the battery discharging or charging operation, respectively. For readability reasons in Fig. 2(a) the areas of operation of the storage system are reported as bold numbers together with X_{CHARG} and X_{DISCH}.

Based on the formulation of the parameters (X_{CHARG}, X_{DISCH}), the partial charge or discharge provided to or by the battery is evaluated as in Eqs. (9), (10) respectively, as suggested by authors in [30]:

$$P_{DISCH\ BATT} = P_{DISCH}\left(1 - X_{DISCH}^3\right)[kW] \tag{9}$$

$$P_{CHARG\ BATT} = P_{CHARG}\left(1 - X_{CHARG}^3\right)[kW] \tag{10}$$

In the equations, P_{DISCH} and P_{CHARG} are the amount of power that would be discharged or charged, respectively, by the battery without these additional criteria, limited by the maximum charge and discharge rate (Eqs. (11), (12)):

$$C_{RATE,C} = 1.0 \tag{11}$$

$$C_{RATE,D} = 2.0 \tag{12}$$

while $P_{DISCH\ BATT}$ and $P_{CHARG\ BATT}$ are the actual amount of power provided to or by the battery both graphically represented in Fig. 2(b). Overall, the concept of this control threshold is to keep the SoC as close as possible to 50 % to improve battery duration and life [29]. The charged or discharged energy is evaluated based on the initial value of power and state of charge. X_{CHARG} and X_{DISCH} are also evaluated based on initial values and do not change during the charging or discharging phase. For example, if the SoC overcomes the OCL or ODL during its charging or discharging, these parameters stay the same. This condition holds true until the SoC goes above UCL or below LDL: in these cases, the charging or discharging is interrupted.

2.2.4. Forced charging

The battery was forced to be charged if its SoC was below 50 % between 2:00 and 4:00 a.m. until 50 % SoC was reached. During this process, power fed into the grid is reduced, so to avoid any RRVs by progressively lowering the power provided to the grid in favor of the one directed towards our storage system (computed as of Eqs. (13), (14)).

$$P_{CHARG\ BATT} = \frac{P_{NOM}}{10} \cdot (\eta_{CHARG}) \; if \; P_i \geq \frac{P_{NOM}}{10} \tag{13}$$

$$P_{CHARG\ BATT} = P_i \cdot (\eta_{CHARG}) \; if \; P_i < \frac{P_{NOM}}{10} \tag{14}$$

This allows to invest in relatively small batteries while at the same time having more energy to provide when needed during the rest of the day.

3. Technical and economic parameters

3.1. Power Ramp Rate: definition and limits

The key parameter when dealing with power smoothing applications is the so-called power Ramp Rate, which quantifies the variation in time of the power produced by a system and is defined as in Eq. (15):

$$RR = \frac{100 \cdot \Delta P}{\Delta t \cdot P_{NOM}}\left[\%\right] = \frac{100 \cdot (P_i - P_{i-1})}{\Delta t \cdot P_{NOM}}\left[\%\right] \tag{15}$$

Power ramp rate calculations are reported graphically in Fig. 3. For grid stability, power ramp rates should be maintained as much as possible inside a certain range, usually based upon a percentage of the wind turbine nominal power (RR_{LIMIT}). While dependent on the local power market regulation standards, in [6] a reference value for this threshold is defined as 10 % per minute (the same is applied also by the Nordic Grid Code and the Puerto Rico Electric Power Authority ([31,32]). This percentage is considered in this work as well.

If the ramp rate exceeds the imposed limits, a violation is committed. From now on, ramp rate and ramp rate violation will be referred to as RR and RRV respectively, for readability reasons.

3.1.1. Economic evaluation of violations

To date, power smoothing methods have been mainly developed at a research level since they are readily not convenient yet, as they require monetary investments (mainly for storage systems), which do not yield any monetary earnings yet as no economic penalties are in place (excluding very few exceptions such as [6]). However, many analysts agree on the fact that future scenarios with higher penetration of intermittent energy production from renewables will likely force countries to make stricter regulations or introduce penalties in case the quality of dispatched power is not in line with expectations. The goal of this study is to support future decisions in this regard by an extended sensitivity analysis comparing different power smoothing methods based on variable levels of economic penalty.

Hypothesized fees have been related to the lack or excess energy provided to the grid when a RRV is committed. Eqs. (16) and (17) report

formulas for both ramp-up and ramp-down violations (RUVs and RDVs respectively).

$$\text{RUV if RR} > 10\% \tag{16}$$

$$\text{RDV if RR} < -10\% \tag{17}$$

In Fig. 4, this behavior is graphically represented, with P_{i-1} and P_i being the power produced during the previous (i-1) and the current (i) minute. Fig. 4 (a) shows a graphical representation of a RDV, since the power P_i decreases more than the allowed value set by the ramp rate limit RR_{limit}. On the other hand, Fig. 4 (b) represents a RUV, when the power P_i excessively increases.

In [6], the penalty for ramp-down ($COST^-$) is valued higher than ramp-up violations ($COST^+$). However, due to the lack of any indication coming from existing regulations, in the present study this penalty has been considered equal for both directions as shown in Eqs. (18), (19).

$$COST^- = penalty \cdot E^- [€] \tag{18}$$

$$COST^+ = penalty \cdot E^+ [€] \tag{19}$$

Where E^- and E^+ are the lacking/excess energy violating the ramp rate limit related to the considered timestep:

$$E^- = \frac{P_{i-1} - |RR_{LIMIT}| - P_i}{60} \left[kWh\right] \tag{20}$$

$$E^+ = \frac{P_i - |RR_{LIMIT}| - P_{i-1}}{60} \left[kWh\right] \tag{21}$$

4. Power smoothing methods

The following section will present the different power smoothing strategies developed and analyzed in the study. These will be benchmarked with respect to a standard configuration that does not involve any kind of storage or additional regulation (referred to as "STD" in the following, for Standard). Then, a simple integration of a BESS is investigated to assess the effectiveness of such systems for the reduction of violations (BAT, for Battery). Next, a method that uses a BESS together with a pitch regulation to always curtail RUVs is investigated (PA+, for Pitch Assisted UP). Lastly, another method that introduces a more active additional pitch regulation is illustrated (PA∓, for Pitch Assisted UP/DOWN). Methods are summarized in Table 1 and further explained in the following.

4.1. STD: uncontrolled base scenario for reference

The STD scenario is the reference upon which the confrontation of the three power smoothing methods presented in this work will be based. This is useful to evaluate how a smoothing method impacts the economic outcome of a wind turbine system when compared to the unruled scenario.

Table 1
Summary of power smoothing methods.

	RRVs	RUVs	RDVs	Added cost
STD	No coverage	No coverage	No coverage	None
BAT	Partial coverage	Partial coverage, via BESS	Partial coverage via BESS	Storage system
PA+	Partial coverage	Complete coverage, via BESS and pitch regulation	Partial coverage, via BESS	Storage system, less energy sold
PA∓	Partial coverage	Complete coverage, via BESS and pitch regulation	Partial coverage, via BESS and pitch regulation	Storage system, less energy sold

4.2. BAT: battery storage system without additional control

As discussed, the first considered power smoothing method consists in the integration of a simple BESS that can be discharged, so as to provide energy when it is needed, or charged when excess power is produced. As in other examples in the literature, no additional regulation is available to cover ramp-up violations even when the storage system SoC is full (or almost full), or when the charging rate limit is reached (partial charge and discharge described by Eqs. (9), (10). In other words, if a RRV is committed, the battery will either charge or discharge, depending on whether it is a RUV or RDV.

With the additional charge/discharge criteria introduced previously, the ways the battery reacts to RRVs can be summed up as follows (see Fig. 2).

If the violation occurs during a power ramp-up:

- Region 2, 3: the battery is charged using all the available excess power, curtailing the RRV and feeding reduced power to the grid.
- Region 4, 5: the battery is charged using a partial amount of the available excess power, lowering the quantity of violating power, but not enough to prevent the RRV. If the amount of energy charging the

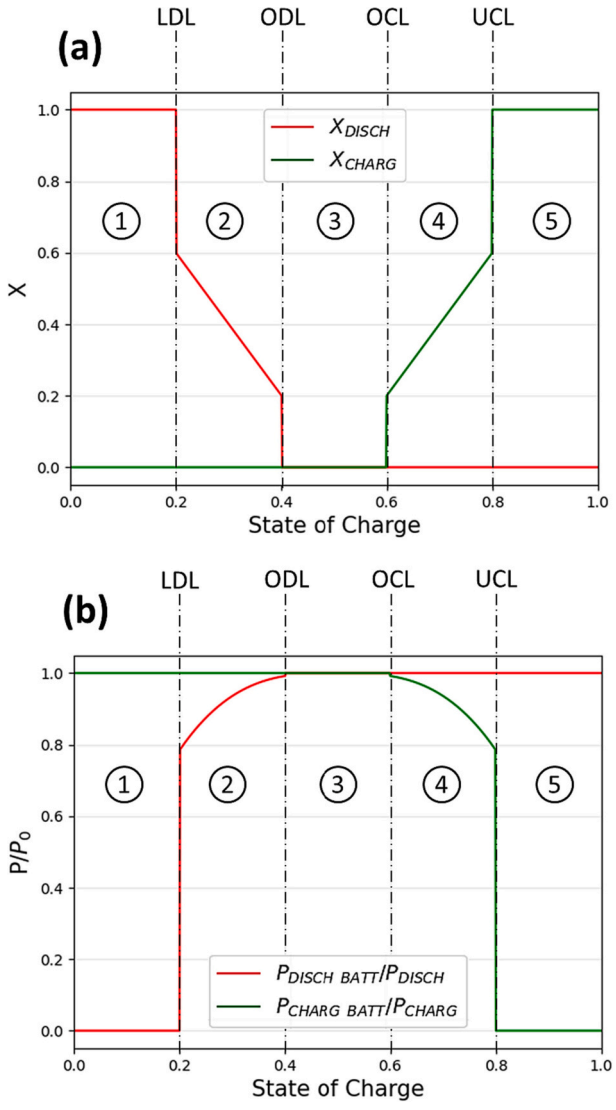

Fig. 2. Modified battery operation parameters depending on its SoC charge/discharge parameters (a), and charge/discharge power ratios (b).

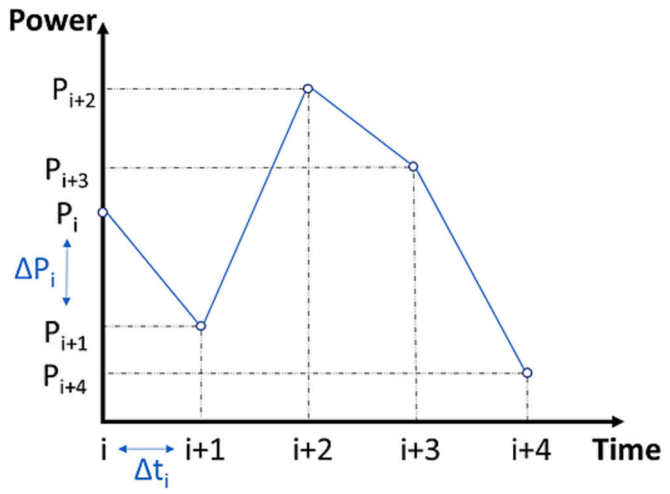

Fig. 3. Graphical example of ramp rate calculations on a small power sample.

battery makes the SoC exceed 80 % (Region 5), charging is interrupted, and the optimal power smoothing is not achieved.

Power evaluations and calculations for RUVs are reported in Eqs. (22), (23):

$$P_{GRID} = P_i - \frac{P_{CHARG\ BATT}}{\eta_{CHARG}} \tag{22}$$

$$P_{CHARG\ BATT} = \left(P_i - \frac{P_{NOM}}{10} - P_{i-1}\right) \cdot \left(1 - X^3_{CHARG}\right) \cdot \eta_{CHARG} \tag{23}$$

where:

- P_{GRID} represents the power output fed to the electric grid after the application of smoothing techniques.
- P_i is the power produced by the turbine at the current minute, calculated as of Eq. (2) with integrated machine data.
- $P_{CHARG\ BATT}$ is the amount of power used to charge the battery.

If instead the violation occurs during a power ramp-down:

- Region 3, 4: the battery is discharged, providing all the needed power, feeding increased power to the grid covering the RRV.
- Region 1, 2: the battery discharges, providing a partial amount of the needed power, lowering the quantity of violating power but not enough to prevent the RRV. If the amount of energy discharged from the battery makes the SoC go below 20 % (Region 1), the discharge is interrupted, not allowing optimal power smoothing.

Power evaluations and calculations for RDVs are reported in Eqs. (24), (25):

$$P_{GRID} = P_i + P_{DISCH\ BATT} \cdot \eta_{DISCH} \tag{24}$$

$$P_{DISCH\ BATT} = \left(P_{i-1} - \frac{P_{NOM}}{10} - P_i\right) \cdot \frac{\left(1 - X^3_{DISCH}\right)}{\eta_{DISCH}} \tag{25}$$

where $P_{DISCH\ BATT}$ is the amount of power provided when discharging the battery.

For the economic calculation, the Net Present Value of the system is used. To this end, excess energy violating the ramp rate limit is first sold with the current energy price, then the penalty is applied.

The flowchart of the control logic is reported in Fig. 5.

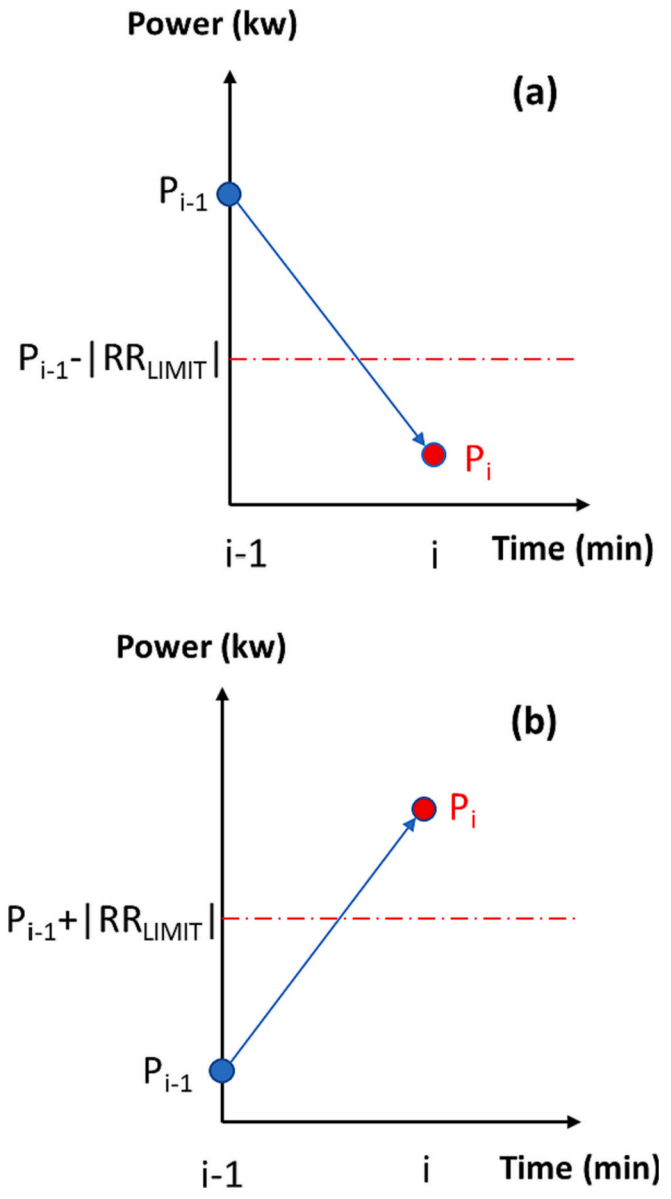

Fig. 4. Graphical representation of a ramp-down violation (a) and a ramp-up violation (b).

4.3. PA+: battery + pitch regulation system for ramp up violations

As discussed, almost all modern utility-scale rotors are equipped with reliable and accurate mechanical systems for adapting the blade pitch angle. Usually, such adaptation is used to regulate the power output beyond the turbine rated speed. However, the possibility of actively regulating power (in relatively short times) is particularly attractive also for combined use with batteries in power smoothing applications to curtail any RRV independently of the battery status or charging C-rate.

The proposed reaction of such combined regulation system to a RUV is as follows:

- Region 2, 3: the battery is fully capable of handling the RUV, thus no action is required to the pitch system.
- Region 4, 5: the pitch system is activated in advance to make sure that the partial charge of the battery defined in Eq. (10) is enough to completely curtail the RUV. If the amount of energy charging the battery makes the SoC exceed 80 % (Region 5), once again the pitch

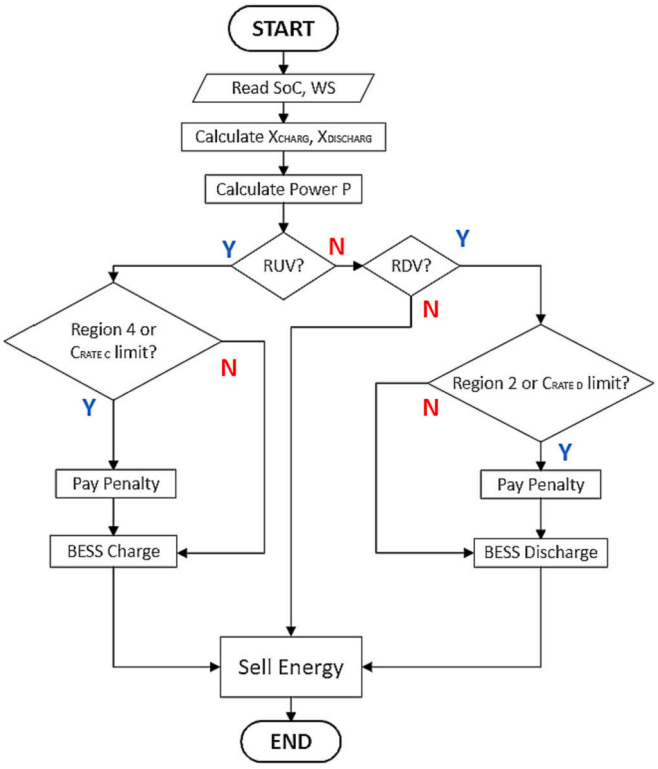

Fig. 5. Flowchart logic of BAT.

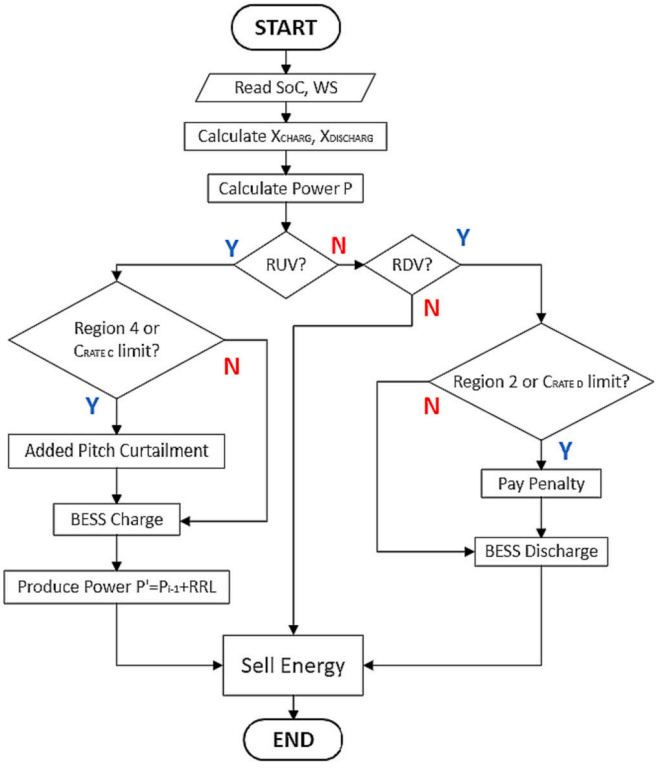

Fig. 6. Flowchart logic of PA+.

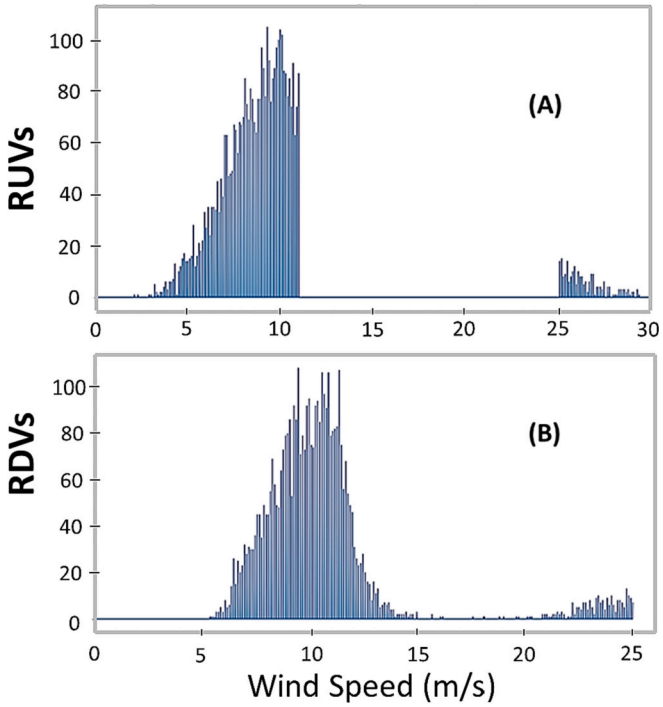

Fig. 7. Ramp-up violations (A) and ramp-down violations (B) at different wind speeds, sample of 02/2015. Analyses related to the non-smoothed configuration.

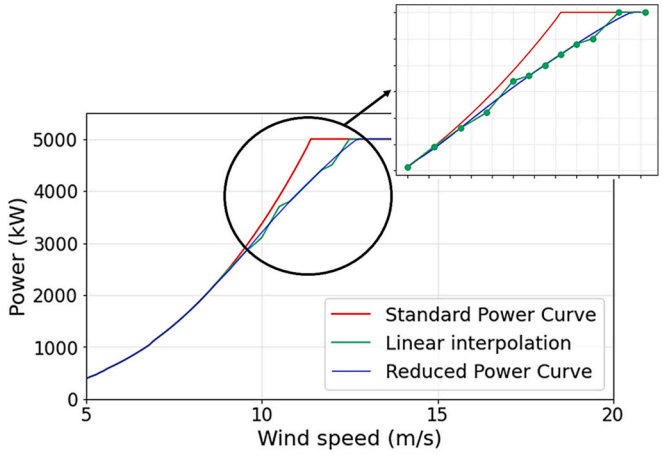

Fig. 8. Example of linear interpolation followed by 5th-order regression to obtain the reduced power curve.

system activates to let the storage system be charged completely, while still removing the RUV.

In the case of a RUV, the power delivered to the grid thus becomes (Eq. (26)):

$$P_{GRID} = P_{CURT,i} - \frac{P_{CHARG\ BATT}}{\eta_{CHARG}} = P_{i-1} + \frac{P_{NOM}}{10} \tag{26}$$

where:

- $P_{CURT,i}$ is the lowered power produced by the turbine with additional pitch, given by Eq. (27):

$$P_{CURT,i} = \frac{1}{2}\eta_{EL}\rho A C_P^{'} V^3 \tag{27}$$

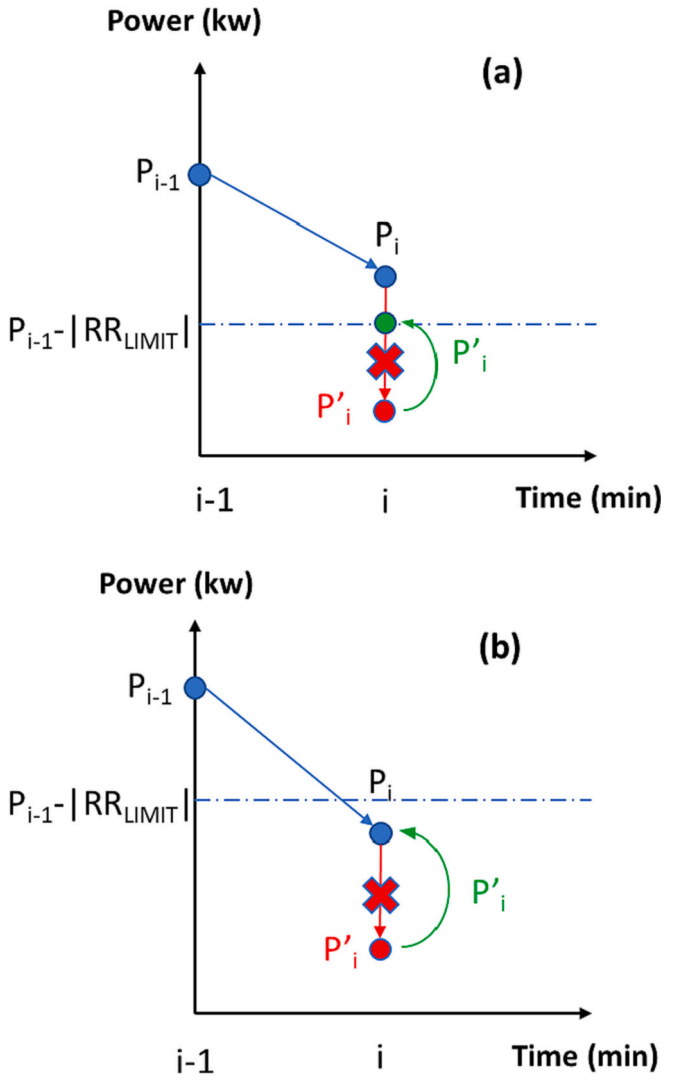

Fig. 9. Additional criteria implemented to avoid introducing RDVs.

- C'$_P$ being the reduced Power Coefficient due to pitch regulation, equal to:

$$C_P^{'} = 2\frac{\frac{P_{CHARG\ BATT}}{\eta_{CHARG}} + P_{i-1} + \frac{P_{NOM}}{10}}{\eta_{EL}\rho A V^3} \tag{28}$$

$P_{CHARG\ BATT}$ is calculated as in Eq. (10).

The behavior for RDVs is analogous to the previous control logic (BAT), and no ramp-down regulation through blade pitch is allowed. The flowchart of the control logic is reported Fig. 6.

4.4. PA∓: battery integration with an adaptive pitch regulation system

The last innovative power smoothing method proposed is the most complex, and differently from the others, aims to regulate directly both ramp-up and ramp-down events through blade pitch action. Similar to the previous method, pitch control is considered together with a BESS to exploit the advantages of both systems. BESS charging is prioritized over pitch actuation whenever possible, to minimize energy waste.

Excluding cut-off events, a RDV can only occur in a wind turbine when the wind speed at the end of the ramp event is below the turbine rated wind speed. In fact, the nominal power curve of pitch-regulated turbine is flat above rated wind speed and therefore no ramp-rate violations can occur. To let the pitch system regulate an RDV, a sufficient amount of power reserve must be maintained. This can be done by considering adding a blade pitch offset or BESS charging, as proposed in this study. In an effort to tailor this control method to the case study at hand, some preliminary analyses are conducted. The goal is to evaluate which wind speeds cause the steeper ramp rates and the highest number of RRVs in this test case, especially RDVs. The underlying idea is that it could be convenient to apply the power curtailment only in this wind speed range.

In Fig. 7, the number of recorded RDVs and RUVs are reported in relation to the wind speed at which they occur (the wind speed reported is relative to the timestep before the RRV). Results show that the most problematic window of wind speed ranged from around 7.5 m/s to 12 m/s, i.e., in a quite narrow range around the nominal wind speed. This can mainly be explained by two factors: at low wind speeds, since the power is related to the cube of wind speed, the power variation related to changes in the resource is smaller. Instead, when above the nominal wind speed the power curve is flat, and violations are unlikely.

Based on the results of Fig. 7, the original power curve of the NREL 5 MW turbine was modified in the range from 8.5 m/s to 13 m/s. The shape of the curve in this region was determined based on an optimization routine. Eight nodes in the power curve were chosen as targets of the optimization. The values of these nodes are top-limited by the nominal power curve and bottom limited by the value of the previous node, as the curve needs to be monotonically increasing (Fig. 8).

The turbine operates according to this optimized power curve when power is following a downward trend (i.e. $P_i - P_{GRIDi-1} < 0$), operating on the nominal power curve otherwise. In other words, the strategy is the same as PA+, combining pitch actuation and battery storage when needed in case of a ramp-up violation, and differs from the latter only when power production is trending downwards.

In addition, for energy waste minimization, the reduction of the power curve is effectuated whenever possible through BESS charging. In this way, energy is partially recovered and not directly curtailed. However, when C_{RATE} or SoC thresholds are exceeded, the power reduction is totally or partially done through pitch regulation. It should be noted that, while the new power curve will reduce the RDVs relative to certain wind speeds, strictly following this power curve may introduce new RDVs in the case of large drops in wind speed. In this case, the power reserve afforded by following the optimized power curve and the BESS is exploited to avoid these violations whenever possible.

To better explain this behavior, in Fig. 9 two examples of possible behaviors in the case of ramp-down violations (Fig. 4(a)) are reported. P'$_i$ is the power fed to the grid at the current minute after the additional pitch regulation or charging process. P'$_i$ is highlighted in red color when no further corrections to the model are applied. The optimized behavior of the PA ∓ system is depicted by green arrows, with P'$_i$ this time highlighted in green color. This is achieved by introducing a set of additional constraints in comparison to the baseline concept described so far (red arrows):

- A reduction of the power fed to the grid via pitching or BESS charging could introduce new RDVs into the system, counteracting the smoothing purpose. Therefore, if the power produced at the timestep "i" (where "i" stands for the present time) by the modified power curve is below the ramp rate limit and would therefore introduce a RDV, while the standard power production is above the limit, the pitch/battery integration works to reduce the power produced until the limit of the admissible ramp rate without introducing a violation is met (Fig. 9(a)).

$$P_i^{'} = P_{i-1} - |RR_{LIMIT}| \tag{29}$$

- If the power produced at the timestep "i" by the modified power curve is below the ramp rate limit and would therefore introduce a

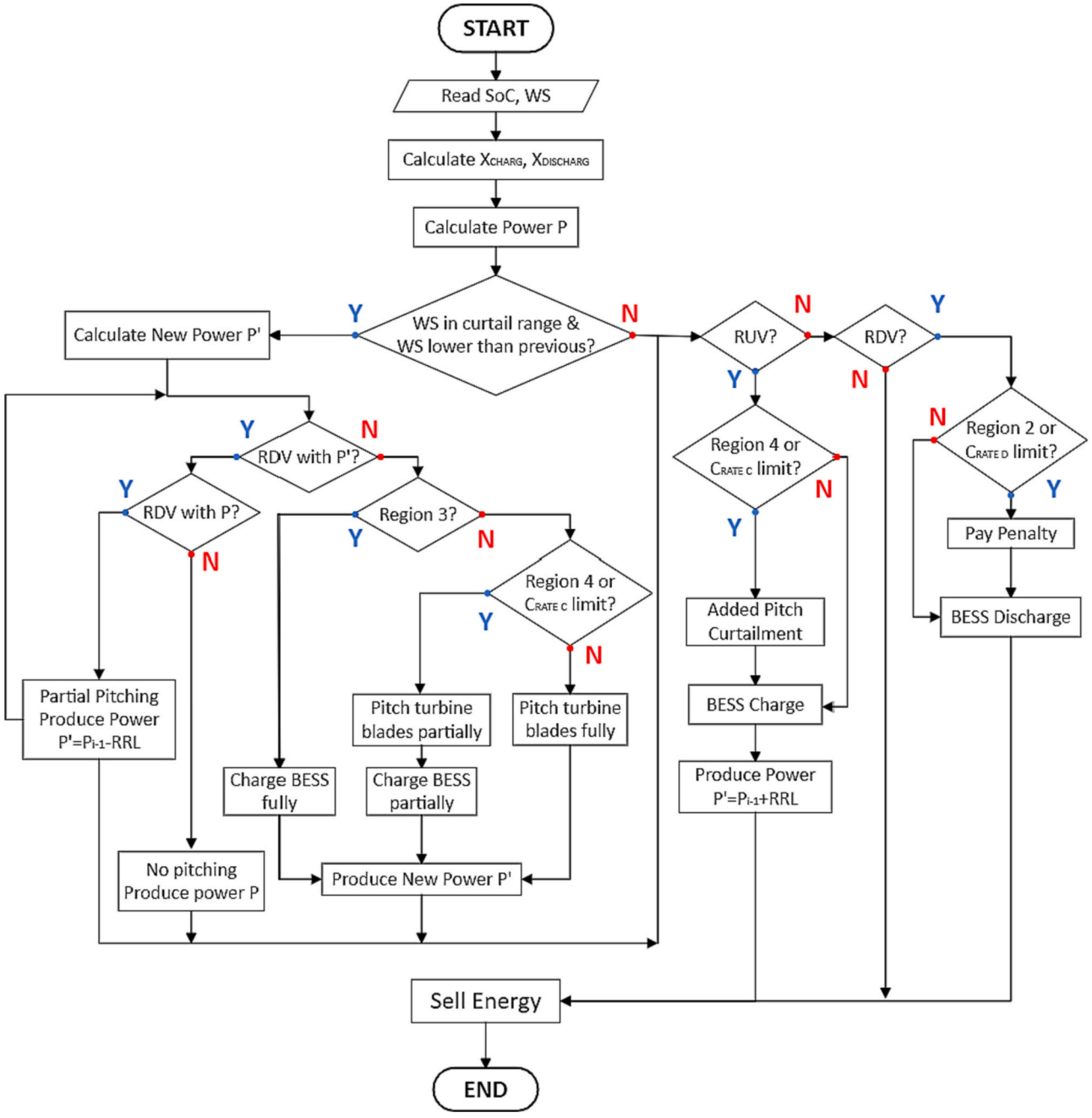

Fig. 10. Flowchart logic of PA $\mp$.

RDV, while the standard power production is also below the limit, the additional BESS charge/pitch regulation is not activated and the turbine follows its standard operation, discharging the battery to cover the RDV if possible (Fig. 9(b)).

$$P'_i = P_i \tag{30}$$

This aims to obtain maximum efficiency and reduce the potential waste of energy that would not increase the power quality of the system. These criteria were chosen over others as they showed economic advantages during preliminary analysis.

The flowchart of the control logic is reported in Fig. 10.

4.5. Optimizer: differential evolution

A multi-parameter optimization was performed to evaluate an economical optimum for each technique:

- For PA+ and BAT, the optimization parameter is the battery size.
- For PA$\mp$, the optimization parameters are nine: battery size and the power values at wind speeds of 9.5, 10, 10.5, 10.8, 11.1, 11.4, 11.7 and 12 m/s used to obtain the modified turbine curve.

The selected optimization algorithm is called Differential Evolution (DE, implemented via the scipy.optimize library). This algorithm, due to Storn and Price [33], finds the global minimum of a multivariate function. DE is stochastic in nature and does not use gradient methods to find

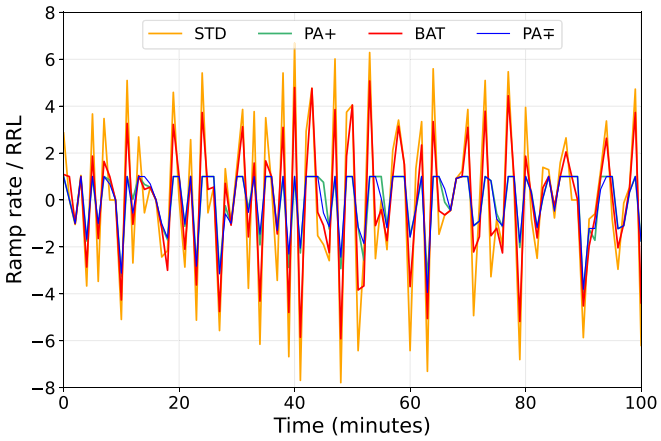

Fig. 11. Power profile sample obtained in different methods (500kWh battery).

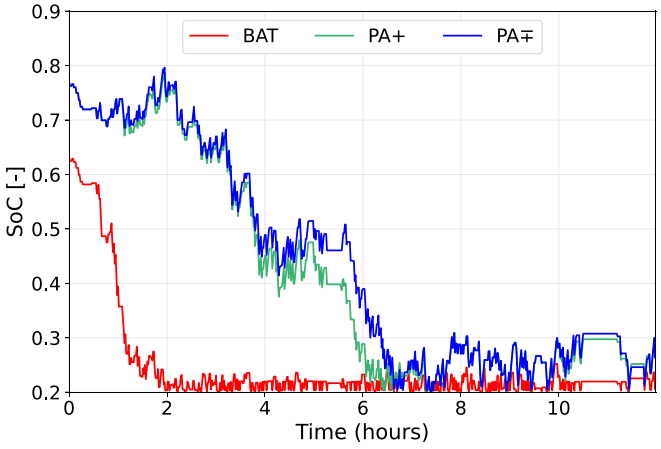

Fig. 12. State of charge sample of the 500-kWh battery under the three control strategies.

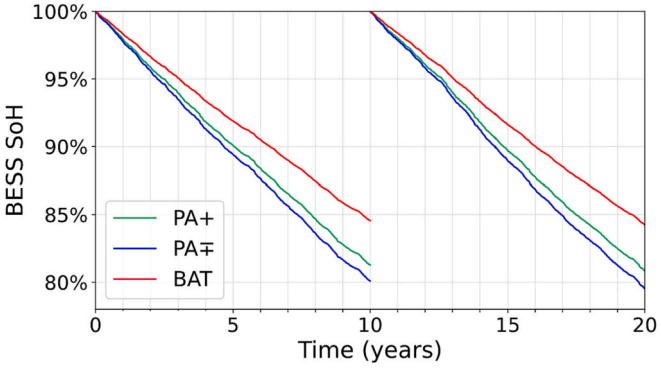

Fig. 13. BESS SoH degradation for various control logics (500 kWh).

the minimum. However, it often requires a larger number of function evaluations than conventional gradient-based techniques. This led to high computational costs, especially for the PA∓ case where nine parameters were optimized. However, being able to locate the global minimum of the objective function was a needed property of the selected optimizer. A preliminary analysis has shown that the objective function to optimize (see following section) is not convex, thus presenting various local minima. Therefore, a gradient-based optimization method would not be able to find the global minimum. With the introduction in our

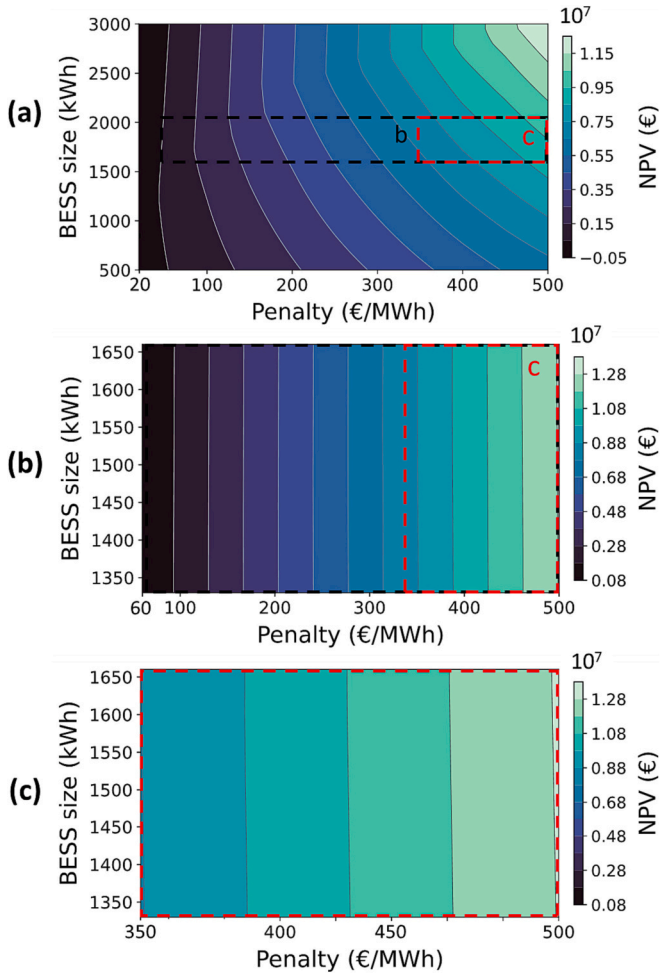

Fig. 14. Differential NPV colormap varying applied penalty and battery size for configurations employing: (a) BAT, (b) PA+, (c) PA∓ in their domain of effectiveness.

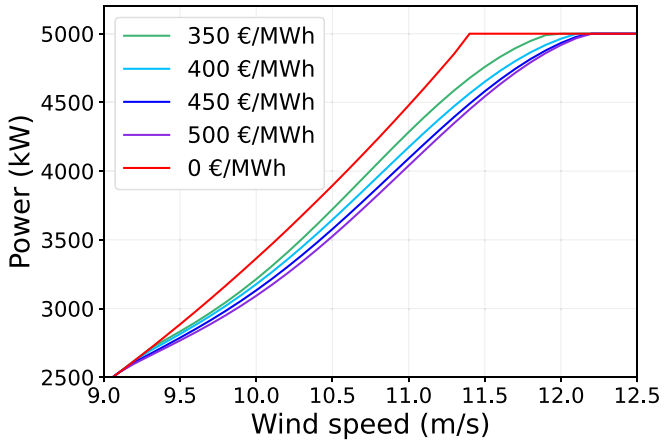

Fig. 15. Deviation of the optimized power curve for different economic penalties.

simulation of DE, this problem was solved as the algorithm can individuate the absolute maximum (as the NPV function goes through a sign change) of the objective function, defined in the following section.

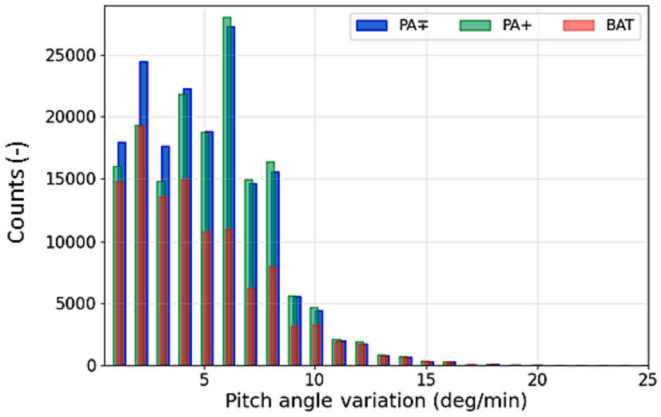

Fig. 16. Pitch angle variation (degree over time) histogram with focus on normal operation.

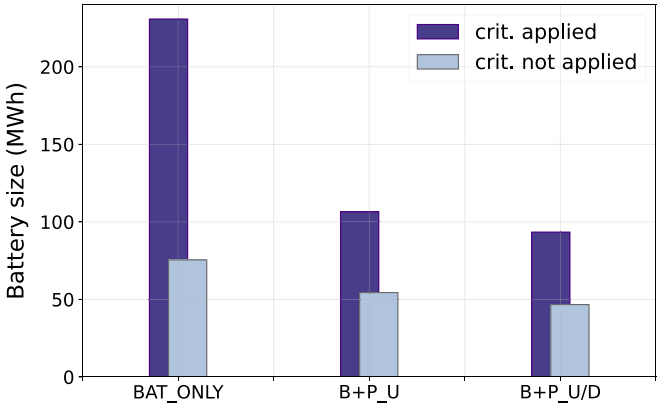

Fig. 17. BESS size needed for no violation, with and without the application of BESS safeguard criterion.

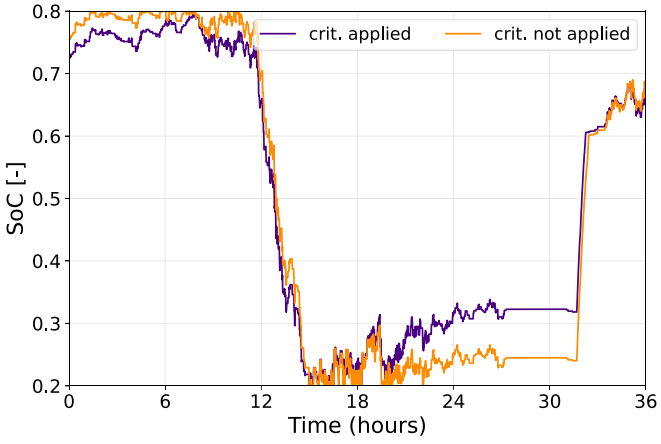

Fig. 18. Different SoC profiles for BAT, with and without BESS safeguard.

4.6. Objective functions

The techno-economic analysis considers a 20-year period, in which the best power smoothing technique is chosen upon the resulting system Net Present Value (NPV), given by:

$$NPV = \sum_{k=1}^{20} \frac{CF_k - CF_{k,PENALTY}}{(int+1)^k} - \sum_{k=0}^{20} \left(\frac{X_k + O\&M \cdot Y_k}{(int+1)^k} \cdot B \cdot C_{BATT} \right) \tag{31}$$

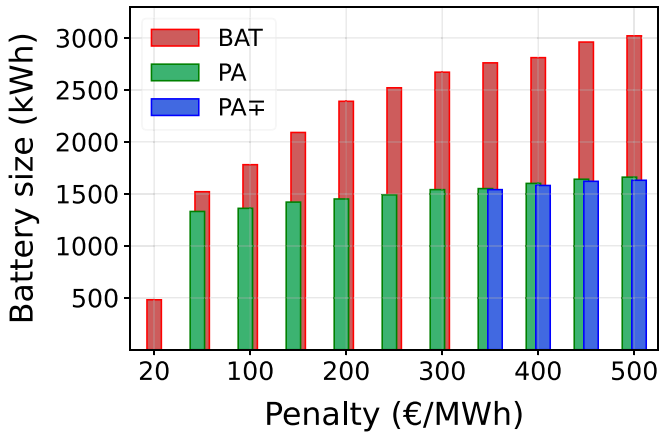

Fig. 19. Optimal BESS size for various methods varying the applied penalty.

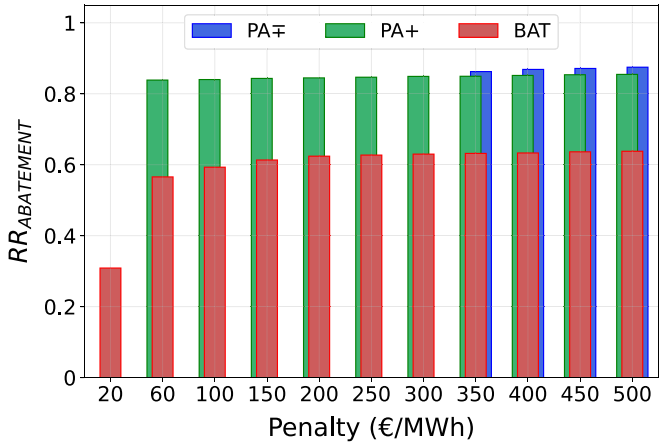

Fig. 20. Ramp rate abatement (%) for different economic penalties.

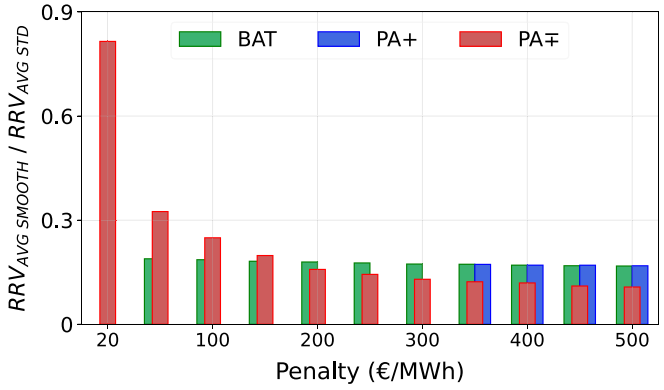

Fig. 21. Ratio of energy violating the ramp rate limit (%) between smoothed and unruled configurations.

Where:

- CF_k is the cash flow of each year, given by the amount of energy sold.

$$CF_k = \sum_{i=0}^{minsyear} \frac{P_{GRID,i}}{60} \cdot PRICE \tag{32}$$

PRICE being energy price in €/kWh, set equal to 0.07 €/kWh ([34,35]) and *minsyear* the number of minutes per year.

- $CF_{k,\ PENALTY}$ is the negative cash flow of each year, given by the amount of energy violating the ramp rate limit:

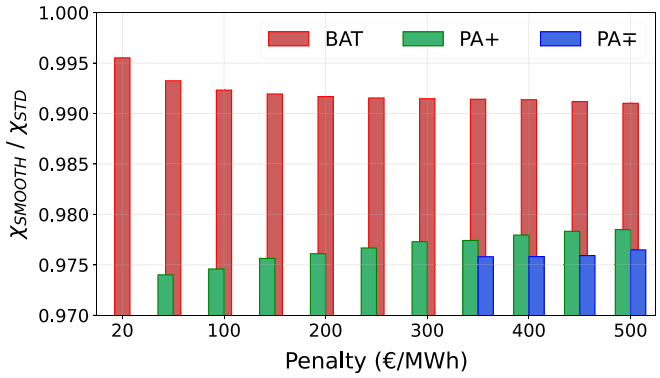

Fig. 22. Total energy sold normalized with respect to the unruled scenario.

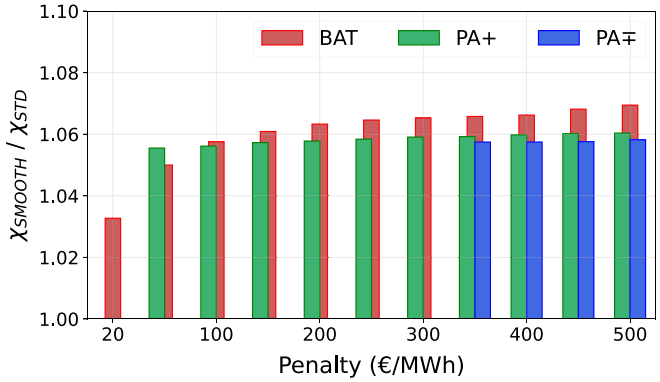

Fig. 23. Produced energy inside the violations' boundaries normalized with respect to the unruled scenario.

$$CF_{k,PENALTY} = \sum_{i=1}^{minsyear} (COST^{+} + COST^{-}) \tag{33}$$

Minute by minute, the cost related to excess/lacking energy is given by Eqs. (18), (19).

- int is the interest rate, corresponding to 5 %
- k is the index relative to the specific year, ranging from zero to twenty
- B is the battery size in kWh
- C_{BATT} is the specific battery cost, in €/kWh, which has been assumed equal to 157.92 €/kWh based on the report in [36]
- X_k is a control variable used to identify the cost fraction relative to a battery change.

  As discussed in Section 2.2.2, if the battery State of Health reaches End of Life (70 %), the battery will be changed with a new one. After ten years, even if the storages SoH has not reached EoL yet, it will be substituted with a new one for safety reasons (this solution was based on industrial experience).

  X_k accounts when and how many times a new cost relative to a new battery was introduced, for every year:
  - o $X_k = 0$ If the BESS is not substituted
  - o $X_k = 1$ If a new BESS is introduced
- Y_k is a control variable used to identify the cost fraction relative to battery operation and management costs. Said costs are applied for every year in which the BESS is not replaced, therefore:

$$Y_k = 1 - X_k \tag{34}$$

- O&M is the cost parameter for the operation and management of the Li-ion battery, equal to 0.02. Due to the lack of concurring data in the literature, this was considered equivalent to a yearly cost of 2 % of the battery CAPEX. This value has been confirmed as reasonable upon discussion with an industrial partner.

Other parameters, for example the turbine cost, are not considered in this analysis as they are equal for any method used, and therefore not relevant for a comparative analysis. Economic optimization has not been further constrained; however, it is forced to respect all the technical limitations imposed to the components.

Finally, an economic scenario has been defined, in which the wind power plant can sell all energy produced, even when a ramp rate violation is committed (this is one of the most credited by analysts in the near future). An economic penalty is however applied based on the violation magnitude by the electrical grid management.

D'Amico et al. [6] reported a penalty of 21.52 €/MWh for RUVs and 26.50 €/MWh for RDVs. However, since to date only a few markets applied similar penalties, a wider sensitivity analysis has been carried out to provide useful information to policymakers, states, and energy providers. Fees ranging from 0 to 500 €/MWh are considered.

5. Results

The main goal of this work is to study the quality improvement of wind turbine power output after the application of smoothing techniques that integrate active pitch control and batteries. More specifically, the configurations resulting from economic optimization for each strategy are compared. Future scenarios in which power fluctuations are penalized through the application of economic penalties are analyzed. This study focuses on power quality, and the methods proposed herein do not focus on smoothing the power fluctuations to avoid the violation from a committed power level, which may also be required of future wind turbines or farms.

The three different power smoothing strategies have been compared from three perspectives. The first one is the impact on the storage system size and health, i.e., evaluating to what extent the batteries can be downsized and used more efficiently. The second perspective is economic competitiveness, i.e., by evaluating the possible economic benefits that the introduction of an active pitch control to support power smoothing can have. The last perspective is power quality, i.e., the overall capacity of the different approaches to mitigate power fluctuations of power delivered to the grid. Proper metrics regarding power quality used in the study are reported below:

Ramp Rate Abatement (RR_{ABAT}): the abatement ratio achieved after the application of a certain control strategy. It is computed (Eq. (35)) as the ratio between the number of ramp rate violations after the application of the control strategy ($RRV_{SMOOTHED}$) and the number of ramp rate violations of the unruled configuration ($RRV_{UNRULED}$).

$$RR_{ABAT} = \left(1 - \frac{RRV_{SMOOTHED}}{RRV_{UNRULED}}\right) \tag{35}$$

Average Ramp Rate Violation Intensity (RRV_{AVG}): average power quantity violating the limit. RRV_{AVG} is computed as the ratio of all the violating power ($POWER_{RRV}$) and the number of violations (RRV).

$$RRV_{AVG} = \frac{POWER_{RRV}}{RRV} \tag{36}$$

Total Amount of Sold Energy (E_{TOT}): total amount of energy sold.

$$E_{TOT} = \sum_{i=0}^{minsyear} \frac{P_{GRID,i}}{60} \tag{37}$$

Non-Violating Energy (χ): the total amount of sold energy E_{TOT}, minus the energy violating the ramp-up limit E_i^+ (computed as of Eq. (38)).

$$\chi = E_{TOT} - \sum_{i=0}^{minsyear} E_i^+ \tag{38}$$

5.1. Preliminary technical validation

Fig. 11 reports a sample of the power production trend under the three control strategies when introducing a 500-kWh battery into the system and can be used to analyze the impact of the smoothing strategy on storage system size and health. In detail, what is reported in Fig. 11 is the ramp rate at every minute (computed as of Eq. (15)) normalized with respect to the ramp rate limit (reported in Eqs. (16), (17)). As explained in Section 4.4, in case of the PA∓ strategy the turbine operates on a different power curve, which is in turn a result of an economic optimization, as discussed in detail in the following. It can be noticed how the BAT strategy provides the least power smoothing, with PA∓ and PA+ being the best and second best, respectively. Compared to BAT, PA+ offers a smoother power to the grid due to its capability of always handling ramp-up violations even when exceeding the charging C_{RATE} or state of charge upper limits of the battery. For PA∓, an even better smoothing is observed; this is due to the combination of pitch regulation and additional battery charges which provide more energy to discharge during the system operation when a ramp-down violation is encountered. The additional charges are afforded by the fact that the system is forced to follow a reduced power curve when the power output is trending downwards in the PA∓ strategy, feeding excess energy into the BESS, as explained in Section 4.4.

The battery state of charge time-series, extracted from the simulated dataset with a battery size of 500 kWh, is shown in Fig. 12. A decreasing SoC can be noted for all three power smoothing strategies, as a result of two main factors. Firstly, an asymmetric C_{RATE} limit is imposed (Eqs. (11), (12)). As a result, in case of high-intensity power ramps the battery discharges faster than it can be recharged. Secondly, because of charge and discharge efficiency, the battery needs to provide more energy than that required to avoid a ramp-down violation but vice-versa can absorb less energy than that required to avoid a ramp-up violation. Consequently, considering that the energy content of ramp-up violations is very similar to that of ramp-down violations in the analyzed time series, the BESS tends to discharge over time. With all of this considered, as shown in Fig. 12, the BESS is heavily under-sized for the BAT method in this preliminary run. On the other hand, the other two methods are able to curtail ramp-up violations even when higher than the charging C_{RATE} and provide a smoother power profile, therefore requiring less stored energy. Fig. 11 graphically represents this: when a RUV and a RDV subsequently take place, PA+ and PA ∓ are able to reduce the power difference by always curtailing the power peak. This allows for reduced energy discharge in the following ramp-down violation, providing an average higher state of charge overall. Among the two pitch-assisted techniques, PA ∓ offers a slightly increased state of charge because of the reduced power oscillations (shown in Fig. 11) and the more frequent battery charges due to the power curve reduction, as previously explained. From the previous considerations, the optimal BESS sizing is expected to be much greater for BAT than the other two methods, which will present a similar optimal battery size (with PA∓ being the smallest overall).

Lastly, the application of the different control logics also influences battery degradation. The economic aspects of said degradation are already calculated in the net present value, since a faster decrease in the state of health of the battery may lead to a premature substitution of the component, which translates into higher operating costs for the system. In particular, it is interesting to note that, when economic considerations come to play, a larger battery that allows for replacement once every 10 years is preferred (so as to save the capital cost of a new unit). Larger batteries tend to undergo working cycles with a smaller depth of discharge that, at least accordingly to empirical degradation models as the one employed here, have a much smaller impact on the lifetime of the device. Taking a closer look to degradation profiles, Fig. 13 shows the decaying of the state of health of the battery during the 20 years of operation, including its planned substitution after 10 years, following the criteria mentioned in Section 4.6. The steeper degradation trend relates to the PA∓ strategy. Even if the power profile delivered is the smoothest among all methods, the more frequent charge and discharge cycles of the battery degrade the battery faster. BAT shows the lowest degradation out of all methods; while this may appear as a positive aspect, it is strictly due to the much lower average SoC (Fig. 12), that limits the battery usage.

5.2. Economic optimization analysis

Following the technical validation of the methods effectiveness, this section compares the Net Present Value of the system after 20 years, calculated by accounting for a variable level of economic penalties set by the grid manager. The analysis is also complemented by a limit scenario, in which it is hypothesized that no ramp rate violations are allowed. This scenario is quite unlikely to happen, especially in highly industrialized countries that will develop smart grid architectures, but it sets a clear asymptote for the evaluation of power smoothing methods.

Fig. 14 shows the highest NPV after 20 years of operation of the best configuration achievable with each of the smoothing methods, varying the economic penalty. The differential NPV reported is computed as the difference optimal NPV of the method and the NPV of the STD configuration, considering the same penalty. Colormaps reported in Fig. 14 allow to plot contemporarily different penalty levels and BESS size ranges. Bright green areas represent the highest net present value, thus the most economically convenient configurations, while dark blue areas represent the lowest NPV. To avoid redundant data, the different control logics were studied only starting from the penalty threshold of absolute convenience. BAT, PA+ and PA∓ are shown in Fig. 14(a), (b) and (c), respectively. Reduced domains are graphically represented by the black dashed line for PA+ and red dashed lines for PA∓ in Fig. 14(a). Black dashed lines highlight the areas of NPV convenience of PA+ compared to BAT, while red dashed lines enclose the areas of NPV convenience of PA∓ compared to PA+.

Upon examination of the results, one can note that:

- below the threshold of around 20 €/MWh, STD operation is the most convenient (i.e., it is economically convenient to accept some economic penalty in response to power fluctuations that cannot be smoothed) as the differential NPV (Fig. 14(a)) is negative.
- between 20 kWh and 60 €/MWh, a simple battery integration without additional curtailments brings the best economic results (BAT).
- if the penalty for ramp rate violations ranges from 60 €/kWh to around 350 €/MWh, the method that presents the highest net present value after 20 years is a combination of an active pitch control with a battery to make sure that ramp up violations are always covered (PA+). Even in a scenario that considers an economic penalty that is slightly lower than the energy selling price, this technique becomes the most convenient power smoothing method. This is due to the benefits of having an overall smoother power production profile.
- for values above 350 €/MWh, the control strategy that employs pitch regulation to reduce the wind turbine power curve together with the previously mentioned storage system (PA∓) becomes the most convenient, albeit very marginally. As mentioned in Section 4.4 the reduced power curve that the turbine follows when this power smoothing strategy is employed is determined based on an economic optimization, which is repeated for each of the considered penalties. As a result, below the threshold of 350 €/MWh, the power curve resulting from this control configuration tends to be very close to the normal configuration, and thus little difference between the two power smoothing strategies can be noted. However, above this value, this strategy allows for increased power smoothing and reduced battery sizes, bringing economical convenience when compared to other methods.

The new optimized power curves of the wind turbine are reported

below (Fig. 15), for values of economic penalties above the convenience threshold (from 350 €/MWh up to 500 €/MWh) of PA ∓ method.

The applied deviation to the power curve with respect to the design one is as expected sensitive to the economic penalty. At the maximum cost applied of 500 €/MWh, the difference between the power node at the rated wind speed and the rated power itself is about 11 % less. While not insignificant, this value is expected to not bring any impactful changes to the turbine standard operation and pitch actuators. A preliminary estimation of the pitch utilization increment was made by reversing the performance maps of the NREL 5 MW turbine. Those maps were used to calculate the total rotation angles of pitch motors binned in terms of magnitude (deg/min) (Fig. 16) for the three scenarios, where the BAT one represents the "normal" pitch use, i.e., the one normally applied for turbine regulation without accounting for power smoothing. To preserve readability, only one year of data is reported, values are clustered into bins of 1°, and the pitch variation to switch off the turbine near the cut-off is neglected.

Upon examination of the figure, it can be observed that almost no increase in pitch use is introduced with the new methods both for conditions of small pitch variation per minute (0°-4°) and for large ones (10° and beyond). These ranges correspond to the normal control of the turbine, i.e., when pitch is used to fine-regulate power along the power curve or to control the power above rated, thus they are perfectly within the range of applicability of actuators in use. A slightly higher increase in pitch variation at very low angles (1–3°/min) is shown for PA ∓ method: this is a consequence of pitching to reduce the wind turbine power curve (Fig. 15). Most of the increase in pitch use (up to +50 % for some bins) is instead seen in the range 4°-10°/min for both the PA+ and the PA ∓ approaches in virtue of the additional use to curtail RUVs below nominal power. By aggregating data from Fig. 16, the number of pitch activations in PA+ and PA+/− is higher of about +47 % and + 53 %, respectively, than that in normal functioning. Although this represents a significant increase in activations, control techniques that are already in use in the industry, such as peak shaving, and/or installation in more gusty sites already imply a number of activations higher than the baseline configuration in the present study. As discussed, however, a more precise estimation should be obtained with a complete aero-servo-elastic model of the rotor, where the pitch-controller can constantly vary blade pitch to control power output and the imposed ramp-rate limitations. Nevertheless, the increased pitch actuation will undoubtedly increase wear on components such as pitch bearings and motors. However, more research is needed within the wind energy community to fully understand the implications of such wear, and to develop simplified models – currently unavailable based on an extended survey made in preparation of this study - that are suitable for simplified models such as the one presented in this study.

An additional point in favor of this configuration is related to the aerodynamic loads on the wind turbine structural components. These loads are stronger when wind speeds approach rated wind speed, and a pitch-to-feather regulation like the one utilized here mitigates said stresses. Indeed, applying a certain amount of blade pitch near rated wind speed to reduce aerodynamic loads is a strategy commonly referred to as "peak shaving" [37].

Another key result obtained from the previous analyses is related to the trend of the NPV resulting from the application of various techniques. As shown in Fig. 14, the implementation of any kind of power smoothing into the system and the optimization of its configuration influence the negative NPV trend in two main ways. First, the isolines shown in Fig. 14 show less dependence of the NPV on battery size when blade pitch power smoothing is introduced. Secondly, among all the power smoothing methods, BAT is the least robust one, as highlighted by the steeper isolines slope. Although this is in part due to the fact that the pitch-assisted power smoothing techniques are economically viable only for a smaller range of battery sizes and penalty values, less variation in NPV for the pitch-assisted methods can be seen even if limiting the comparison to their respective design spaces. Among pitch-assisted methods, PA∓ presents the least NPV sensitivity to penalty values, although the difference is extremely marginal when compared to PA+ in the reported penalty range. However, PA∓ becomes increasingly more convenient in the long run, thanks to the possibility of optimizing multiple working parameters.

5.2.1. No-violations scenario

It is interesting to understand the potential limits of the proposed power smoothing strategies to analyze a limit scenario in which no ramp rate violations are allowed by the grid. Moreover, this scenario is also used as a test bench to highlight the effects of the battery protection criterion described in Section 2.2.3. Optimal battery sizes in this scenario are reported in Fig. 17: as predicted earlier (Fig. 14), the best results are obtained with PA∓ method. It can be noticed how PA∓ control strategy allows for the lowest BESS and investment when compared to other methods, thanks to the possibility of curtailing the power curve and providing more power to charge the battery. Comparing PA+ and BAT in Fig. 17, the former provides reduced optimal BESS sizing, once again thanks to the additional pitch curtailment. When no penalties are allowed, due to the huge battery capacities observed, the charging C_{RATE} is not a limitation anymore: therefore, the benefits come both from the smoother power profiles and the possibility of curtailing ramp-up violations even for high states of charge.

Focusing now on the safeguard criteria explained in Section 2.2.3, as expected its introduction yielded to a higher battery size, as the goal of this scenario is to remove any ramp rate penalty during the 20-year timeframe. Moreover, if we compare runs with and without the battery safeguard criterion in Fig. 17, the economic optimum is reached for much larger battery capacities when no safeguard criterion is used. This is especially noticeable when no pitch assistance is used. The reason is explained in Section 2.2.3: when the safeguard criterion is applied, the SoC must be comprehended between the 40 % and 60 % limit to fully cover the RRV. This sets a need to invest in a much greater capacity BESS so that SoC oscillations are reduced.

The results shown in Fig. 17 are clearly in favor of not using the safeguard criterion. In a more realistic scenario, however, this strategy has shown itself to be effective. In fact, in Table 2, the techno-economic outcomes of the application of BAT method with and without the battery safeguard criteria are compared, considering a scenario of 40€/MWh penalty with a 1200 kWh battery (optimized sizing). Results show that the removal of the safety criterion greatly reduces ramp rate violations, but their average intensity is much higher. The system is indeed capable of completely smoothing more violations, but those that cannot be smoothed are of much higher intensity. In addition, both the energy sold during the 20-year period and the energy produced respecting the violation boundaries are lower after the removal of the safeguard criterion. This highlights how completely removing fewer violations but still greatly reducing their intensity proves to be a more viable choice, since economic penalties are calculated based on the energy that is sold to the grid in violation of the RR limits, and not based on the number of RR violations. As a result, even the net present value is higher, although slightly, proving the algorithm effectiveness.

The effects of the criterion are shown in Fig. 18, which compares the state of charge trend with and without the application of the safeguard criterion in the scenario described in Table 2. The criterion effectively limits the variation of the state of charge. Particularly, it can be shown how the state of charge is increased when approaching its lower limit and reduced when close to its upper limit: this creates a buffer to provide the option of charging or discharging the battery as often as possible.

Table 2
Effects of safeguard criterion on BAT (40 €/MWh penalty, 1200 kWh BESS).

	RR_{ABAT}	RR_{AVG}	E_{TOT} (MWh)	χ (MWh)	NPV (€)
Crit. yes	55 %	48 %	17'281'084	16'998'604	11'999'446
Crit. no	**77 %**	97 %	17'278'895	16'989'667	11'993'144

This allows to partially or completely smooth a ramp rate violation that would take place without the introduction of the BESS safeguard criterion. Therefore, based on results reported in Table 2 and Fig. 18, the safeguard criterion is integrated in both previous and following analyses.

5.2.2. Optimal sizing of the battery energy storage system

Following the NPV colormap shown in Fig. 14, the optimal battery sizing for every penalty and every method studied are reported in Fig. 19. The optimal battery capacity grows when the penalty increases, with different sensitivity to the penalty depending on the method.

Results obtained follow the expected trend predicted in Fig. 12; the BAT technique must rely on high-capacity batteries to face high penalties. This is because the system, under that control strategy, can only increase the battery size to reduce the number of ramp rate violations and their intensity, which at penalty values higher than the energy selling price are never economically convenient. This behavior changes when other methods are applied, since the additional pitch curtailment also helps with the reduction of ramp down violations, and the same effect can be obtained with smaller battery sizes. This is apparent if one considers penalties slightly higher than the energy price. In such a scenario, optimal sizing of the battery is reduced by around 13 % to 45 % depending on the penalty when integrating pitch curtailment for power smoothing. PA+ and PA∓ applications report very similar results in terms of optimal battery sizing, with the latter having optimal battery capacity slightly reduced (−3 % at most). This reduction is once again due to the smoother power profile and additional charges.

5.2.3. System power quality

Results from the previous section highlighted how, from the point of view of the wind park owner, the choice of optimal control method is strictly dependent on the economic penalty introduced in the system.

This section analyses the power quality that is achieved with the application of the control strategies. To this end, Ramp rate abatement (RR_{ABAT}) is one of the most used parameters to analyze power quality improvements. Fig. 20 reports the resulting RR_{ABAT} coming from the optimal application of the different control strategies over a wide range of penalties. Results show that methods that involve an active pitch control are characterized by an optimal ramp rate abatement ranging from 84 to 88 %, with PA∓ reducing the number of violations the most. On the other hand, when only a battery is utilized to avoid violations (BAT), it becomes economically convenient to allow many more violations and the resulting RR_{ABAT} ranges from 31 % to only 64 %. To reach comparable ramp rate abatements with BAT, the price of a large-capacity battery would imply a huge investment cost that cannot be recovered during the lifetime of the asset.

Fig. 20 shows that, even when high economic penalties are applied, the ramp rate abatement is fast saturating and limited to lower values than other literature results (i.e., [8]). The reason for this lies in the introduction of the safeguard criterion proposed in Section 2.2.3: with the implementation of the criterion, a ramp rate violation can be removed only for a limited range of the battery state of charge. As mentioned in Section 5.2.1., the criterion was implemented for positive effects observed on power quality, energy sold, and NPV.

The absolute number of violations abatement alone is not enough to evaluate the power quality improvement. Indeed, the intensity of the ramp rate violations and the magnitude of the energy that violates the imposed boundaries is another key metric to consider. Fig. 21 shows the ratio between the average value of the ramp rate violations (RRV_{AVG}) committed under the three control methods and the unruled one. PA+ and PA∓ provide low values even for low battery size and low penalty scenarios (17–19 %). On the other hand, the strategy that only relies on the battery (BAT) presents comparable reductions only when much larger storage systems are utilized (battery size over 2 MWh, Fig. 19). It can be observed that, differently from the ramp rate abatement, the intensity of the violation is less sensitive to the applied method and more sensitive to the BESS size. At extremely high penalties (200–500 €/MWh), the BAT strategy leads to greater abatements in ramp rate intensity than with other smoothing methods (minimum of 11 %). In short, this strategy leads to substantially more ramp rate violations (Fig. 20), which are slightly less intense on average (Fig. 21). However, this approach remains not convenient from an economic point of view, being the net present value lower than with other methods due to the introduction of such a large storage system.

Results reported in Fig. 20 and Fig. 21 show that from a grid operator point of view, increasing the penalty above 60 €/MWh (slightly lower than the energy selling price) brings next to no benefits to the system power quality, both regarding the number and intensity of ramp rate violations. From the plant owner's perspective on the other hand, if economically convenient methods are used (PA+ or PA∓), the optimal battery size and reduced power curve observe small variations. Differently, when implementing the BAT techniques, the optimal battery size growth rate shows more sensitivity to the economic penalty increase.

To also value the effective waste of energy coming from the application of different smoothing techniques, the amount of energy sold during the 20-years lifetime is analyzed. Fig. 22 shows the ratio between the energy sold for all the smoothing methods and the unruled configuration "STD".

The energy sold under the unruled control is always greater than in configurations equipped with storage systems, and therefore the energy ratio is always less than one. This is because ramp-up violations are never curtailed nor absorbed in STD, allowing the system to sell more energy. For BAT, the implementation of a simple battery without curtailment provides the highest values of the parameter among the other methods. Although with less excess energy than STD because of the storage system. When increasing the BESS size, more ramp-up violating energy is absorbed instead of directly sold to the system and is thus subtracted from the BESS round-trip efficiency before being sold to the grid, which explains the slightly downward trend. On the other hand, the application of active pitch control to smooth the power profile inevitably reduces the generated energy from the wind turbine. Compared to BAT, an inverse trend of the parameter can be observed in the pitch-assisted methods. This is due to the increase of the optimal battery size increase, which implies less energy curtailed via pitch.

However, the absolute value of the sold energy is not sufficient to evaluate the effectiveness of one method over another. In certain scenarios, excess energy could be curtailed and may not produce revenues for the producer. To further analyze this aspect, the energy not violating the ramp rate limit (χ) was introduced (Eq. (38)) and computed for the analyzed control strategies. All three power smoothing strategies are able to increase the energy that is sold to the grid without incurring an economic penalty (Fig. 23). In particular, with the PA+ and PA∓ smoothing techniques, the produced energy that respects the imposed

Table 3
Techno-economic comparative analysis for the three different methodologies.

Penalty (€/MWh)	E_{TOT} (GWh)	Battery Investment (k€)	Battery Replacement (k€)	NPV (k€)
		BAT		
20	17′335	76	47	12′184
60	17′269	240	147	11′904
350	17′255	436	268	11′352
500	17′254	477	293	11′203
		PA+		
60	16′961	210	129	11′920
350	17′020	245	150	11′694
500	17′039	262	161	11′589
		PA∓		
350	16′992	243	149	11′701
500	16′997	257	158	11′612

boundaries increases by roughly 6 % when compared to the unruled configuration. Moreover, the latter reports a lower amount of energy sold once again due to the more aggressive implementation of pitch curtailment. The increment brought by the method that only relies on the battery is more sensitive to the applied penalty and ranges from 3 % to 7 %. This is once again due to the sensible increase of the optimal BESS size in the penalty range analyzed. Compared to Fig. 22, χ is increased when the penalty grows because the bigger battery is able to provide more energy inside the ramp rate constraints. Techno-economic results discussed so far are summarized in Table 3, for the three power smoothing methods and in the penalty ranges of economic convenience.

6. Conclusions and future developments

In this study, an investigation of the impact that different power smoothing techniques could have on the techno-economic outcome of a wind farm is performed. The objective of the methods that are proposed and analyzed is to improve the power quality and stability of the grid by reducing the amount and intensity of ramp rate violations while limiting the economic impacts of the system. The case study for comparative analyses comprehends a Li-Ion battery system and a single utility-scale, multi-MW wind turbine (NREL 5 MW reference wind turbine). While developed for a single turbine, however, the methodology is ready to be replicated for an entire farm, in combination with additional targets at farm control level, as will be discussed later in this section. Wind data used consist of a one-minute synthesized database of real anemometric measures from Kedros (Greece).

Two innovative power smoothing techniques are proposed, both based on the integration of blade pitch regulation with a standard battery. Although the use of blade pitch for power quality in addition to conventional control is not new, the combination proposed herein with the batteries and incorporating novel criteria for the safeguard of their state of health is totally novel. Moreover, these methods are analyzed focusing not only on technical implementation, but also on the economic effectiveness of the system, thus looking for a techno-economic optimization of each solution.

More specifically, in PA+, the additional pitch regulation is introduced to ensure that no ramp-up violations are committed even if the storage system is unable to store the excess energy. In PA∓, pitch curtailment is also used to reduce the power produced for a certain range of wind speeds to smooth the power output variation. After analyzing the phenomenology of the ramp rate violations, this range was chosen to determine which wind speeds were most problematic for power fluctuations. Preliminary comparative analyses showed how innovative methods provided an average battery state-of-charge higher than a simple BESS integration and a smoother power profile.

The results of a multi-parameter optimization were analyzed under three perspectives, i.e., economic convenience, effectiveness of the storage system usage, and power quality. Since no agreement is currently found on the most suitable regulatory strategy to manage power violations in electrical grids worldwide, several scenarios are studied. Economically focused results show how the different specific economic penalty applied for each kilowatt-hour of excess/lacking energy is the key parameter that will determine the most convenient configuration in the future. More specifically:

- below 20 €/MWh, the most convenient configuration is the unruled one (STD) and the applied penalty does not justify an investment in a battery or the additional energy curtailment of active pitch control for power smoothing.
- between 20 €/MWh and 60 €/MWh, it is convenient to integrate a battery in the system for power smoothing purposes with no additional pitch curtailment (BAT).
- between 60 €/MWh and 350 €/MWh, the most convenient configuration combines a BESS with an active pitch regulation that covers all the ramp-up violations (PA+).
- above 350 €/MWh, modifying the power curve of the wind turbine via pitch control to create a power reserve to cover even the ramp-down violations becomes convenient (PA∓).
- in a scenario where no ramp rate violations are allowed, PA∓ provided the best economic results with the lowest BESS size and investments.

Focusing, however, on the quality improvement of wind turbine power output, abatement ratios for proposed innovative methods range from around 84 % to 88 %, and the average intensity of those violations is reduced to around 17–19 % compared to a standard operation. The PA∓ method provides the best smoothing capability, although just slightly above PA+. Differently, the use of a battery only (BAT) provides the lowest ramp rate abatement ratio (31 % to 64 % at most) due to the inability of absorbing excess energy in the mentioned circumstances. In general, while the implementation of the battery safeguard criterion yielded low ramp rate abatements, violation intensities were greatly reduced and more energy was sold over the 20 years, increasing the system net present value. From a grid operator's perspective, these results suggest that a future scenario in which the economic penalty is above the threshold of 20 €/MWh justifies the investment cost of a battery, bringing substantial power quality improvements. Even higher benefits are observed up to 60 €/MWh, where pitch-assisted curtailment becomes convenient. However, increasing the penalty above the selling price (70 €/MWh) only brings marginal improvements: this holds true especially if optimal methods (PA+ and PA∓) are applied.

Focusing on the prospects of the proposed methodologies, it is worth remarking that, while the innovative techniques proposed in this study were developed focusing on a single turbine, so as to have a precise overview on all the parameters under consideration, power smoothing also needs to be tackled on a farm level. Applying these techniques to a proper wind farm is, however, a multi-faceted problem and is demanded to further reach on the topic. In fact, many studies such as [8] have shown that the power fluctuations from multiple turbines can in some scenarios balance the farm's power fluctuations. Moreover, the smoothing techniques require rethinking on the farm scale. For instance, one could assign power smoothing duties to one or a small subset of the wind farm's turbines, or apply the techniques discussed herein to all the turbines. Or it may be more convenient to switch between the former and the latter approach depending on the operating condition and instantaneous wind orientation. Finally, different power control targets could also be prioritized such as voiding violations of scheduled/committed power levels of the farm as a whole.

Overall, the study proves that the introduction of additional control logics for power smoothing that can also exploit the embedded blade pitch regulation can provide benefits at all levels in future market scenarios in which ramp rate violations are strongly penalized, or even prohibited.

CRediT authorship contribution statement

Claudio Galli: Writing – original draft, Visualization, Validation, Software, Methodology, Formal analysis, Data curation, Conceptualization. **Francesco Superchi:** Writing – review & editing, Visualization, Validation, Supervision, Software, Methodology, Formal analysis, Data curation, Conceptualization. **Francesco Papi:** Writing – review & editing, Supervision, Software, Methodology, Investigation, Data curation, Conceptualization. **Giovanni Ferrara:** Supervision, Resources, Project administration, Funding acquisition. **Alessandro Bianchini:** Writing – review & editing, Supervision, Resources, Project administration, Methodology, Investigation, Funding acquisition, Data curation, Conceptualization.

Declaration of competing interest

The authors declare that they have no known competing financial

interests or personal relationships that could have appeared to influence the work reported in this paper.

Data availability

Data will be made available on request.

Acknowledgments

This research received no external funding.

References

[1] World Energy Outlook, Analysis, IEA, 2021. Accessed: Jul. 03, 2023. [Online]. Available: https://www.iea.org/reports/world-energy-outlook-2021.
[2] H. Babazadehrokni, 'Power Fluctuations Smoothing and Regulations in Wind Turbine Generator Systems'.
[3] M. Jabir, H. Azil Illias, S. Raza, H. Mokhlis, Intermittent smoothing approaches for wind power output: a review, Energies 10 (10) (Oct. 2017) 1572, https://doi.org/10.3390/en10101572.
[4] M.A. Chowdhury, N. Hosseinzadeh, W.X. Shen, Smoothing wind power fluctuations by fuzzy logic pitch angle controller, Renew. Energy 38 (1) (Feb. 2012) 224–233, https://doi.org/10.1016/j.renene.2011.07.034.
[5] E. Reihani, M. Motalleb, R. Ghorbani, L. Saad Saoud, Load peak shaving and power smoothing of a distribution grid with high renewable energy penetration, Renew. Energy 86 (Feb. 2016) 1372–1379, https://doi.org/10.1016/j.renene.2015.09.050.
[6] G. D'Amico, F. Petroni, S. Vergine, An analysis of a storage system for a wind farm with ramp-rate limitation, Energies 14 (13) (Jul. 2021) 4066, https://doi.org/10.3390/en14134066.
[7] S. Belaid, D. Rekioua, A. Oubelaid, D. Ziane, T. Rekioua, A power management control and optimization of a wind turbine with battery storage system, J. Energy Storage 45 (Jan. 2022) 103613, https://doi.org/10.1016/j.est.2021.103613.
[8] A. Mannelli, F. Papi, G. Pechlivanoglou, G. Ferrara, A. Bianchini, Discrete wavelet transform for the real-time smoothing of wind turbine power using Li-ion batteries, Energies 14 (8) (Jan. 2021) 8, https://doi.org/10.3390/en14082184.
[9] L.M.S. De Siqueira, W. Peng, Control strategy to smooth wind power output using battery energy storage system: a review, J. Energy Storage 35 (Mar. 2021) 102252, https://doi.org/10.1016/j. est.2021.102252.
[10] R. Sebastián, R. Peña Alzola, Flywheel energy storage systems: review and simulation for an isolated wind power system, Renew. Sust. Energ. Rev. 16 (9) (Dec. 2012) 6803–6813, https://doi.org/10.1016/j.rser.2012.08.008.
[11] G.F. Frate, P. Cherubini, C. Tacconelli, A. Micangeli, L. Ferrari, U. Desideri, Ramp rate abatement for wind power plants: a techno-economic analysis, Appl. Energy 254 (Nov. 2019) 113600, https://doi.org/10.1016/j.apenergy.2019.113600.
[12] M. Ammar, G. Joos, A short-term energy storage system for voltage quality improvement in distributed wind power, IEEE Trans. Energy Convers. 29 (4) (Dec. 2014) 997–1007, https://doi.org/10.1109/TEC.2014.2360071.
[13] W. Jing, C. Hung Lai, S.H.W. Wong, M.L.D. Wong, Battery-supercapacitor hybrid energy storage system in standalone DC microgrids: a review, IET Renew. Power Gener. 11 (4) (2017) 461–469, https://doi.org/10.1049/iet-rpg.2016.0500.
[14] P.H.A. Barra, W.C. De Carvalho, T.S. Menezes, R.A.S. Fernandes, D.V. Coury, A review on wind power smoothing using high-power energy storage systems, Renew. Sust. Energ. Rev. 137 (Mar. 2021) 110455, https://doi.org/10.1016/j.rser.2020.110455.
[15] M. Mahmoud, M. Ramadan, A.-G. Olabi, K. Pullen, S. Naher, A review of mechanical energy storage systems combined with wind and solar applications, Energy Convers. Manag. 210 (Apr. 2020) 112670, https://doi.org/10.1016/j.enconman.2020.112670.
[16] A.M. Howlader, N. Urasaki, A. Yona, T. Senjyu, A.Y. Saber, A review of output power smoothing methods for wind energy conversion systems, Renew. Sust. Energ. Rev. 26 (Oct. 2013) 135–146, https://doi.org/10.1016/j.rser.2013.05.028.
[17] T.L. Van, D.-C. Lee, Ouput power smoothening of variable-speed wind turbine systems by pitch angle control, in: 2012 10th International Power & Energy Conference (IPEC), IEEE, Ho Chi Minh City, Nov. 2012, pp. 166–171, https://doi.org/10.1109/ASSCC.2012.6523258.
[18] P. Garasi, M. Watanabe, Y. Mitani, Power smoothing of wind turbine generator using Fuzzy-PI pitch angle controller, in: 2014 Australasian Universities Power Engineering Conference (AUPEC), IEEE, Perth, Australia, Sep. 2014, pp. 1–5, https://doi.org/10.1109/AUPEC.2014.6966531.
[19] E. Hittinger, J. Apt, J.F. Whitacre, The effect of variability-mitigating market rules on the operation of wind power plants, Energy Syst. 5 (4) (Dec. 2014) 737–766, https://doi.org/10.1007/s12667-014-0130-8.
[20] M. Korpas, A.T. Holen, Operation planning of hydrogen storage connected to wind power operating in a power market, IEEE Trans. Energy Convers. 21 (3) (Sep. 2006) 742–749, https://doi.org/10.1109/TEC.2006.878245.
[21] D. Huang, et al., A mixed integer optimization method with double penalties for the complete consumption of renewable energy in distributed energy systems, Sustain Energy Technol. Assess. 52 (Aug. 2022) 102061, https://doi.org/10.1016/j.seta.2022.102061.
[22] H. Chen, J. Chen, G. Han, Q. Cui, Winding down the wind power curtailment in China: what made the difference? Renew. Sust. Energ. Rev. 167 (Oct. 2022) 112725, https://doi.org/10.1016/j.rser.2022.112725.
[23] J. Jonkman, S. Butterfield, W. Musial, G. Scott, 'Definition of a 5-MW Reference Wind Turbine for Offshore System Development', NREL/TP-500-38060, 947422, Feb. 2009, https://doi.org/10.2172/947422.
[24] E. Locorotondo, et al., Electrical lithium battery performance model for second life applications, in: 2020 IEEE International Conference on Environment and Electrical Engineering and 2020 IEEE Industrial and Commercial Power Systems Europe (EEEIC/I&CPS Europe), IEEE, Madrid, Spain, Jun. 2020, pp. 1–6, https://doi.org/10.1109/EEEIC/ICPSEurope49358.2020.9160496.
[25] M.J.E. Alam, T.K. Saha, Cycle-life degradation assessment of Battery Energy Storage Systems caused by solar PV variability, in: 2016 IEEE Power and Energy Society General Meeting (PESGM), IEEE, Boston, MA, USA, Jul. 2016, pp. 1–5, https://doi.org/10.1109/PESGM.2016.7741532.
[26] E. Martinez-Laserna, V. Herrera, I. Gandiaga, A. Milo, E. Sarasketa-Zabala, H. Gaztañaga, Li-ion battery lifetime model's influence on the economic assessment of a hybrid electric bus's operation, World Electr. Veh. J. 9 (2) (Jul. 2018) 28, https://doi.org/10.3390/wevj9020028.
[27] Y. Shi, B. Xu, Y. Tan, B. Zhang, A convex cycle-based degradation model for battery energy storage planning and operation, in: 2018 Annual American Control Conference (ACC), IEEE, Milwaukee, WI, USA, Jun. 2018, pp. 4590–4596, https://doi.org/10.23919/ACC.2018.8431814.
[28] M.A. Abdullah, K.M. Muttaqi, D. Sutanto, A.P. Agalgaonkar, An effective power dispatch control strategy to improve generation schedulability and supply reliability of a wind farm using a battery energy storage system, IEEE Trans. Sustain. Energy 6 (3) (Jul. 2015) 1093–1102, https://doi.org/10.1109/TSTE.2014.2350980.
[29] J. Tan, Y. Zhang, Coordinated control strategy of a battery energy storage system to support a wind power plant providing multi-timescale frequency ancillary services, IEEE Trans. Sustain. Energy 8 (3) (Jul. 2017) 1140–1153, https://doi.org/10.1109/TSTE.2017.2663334.
[30] F. Mapelli, M. Mauri, D. Tarsitano, Energy control strategies comparison for a city car Plug-In HEV, in: 2009 35th Annual Conference of IEEE Industrial Electronics, IEEE, Porto, Portugal, Nov. 2009, pp. 3729–3734, https://doi.org/10.1109/IECON.2009.5415113.
[31] Nordel, Nordic Grid Code 2007, 2007, pp. 69–74.
[32] V. Gevorgian, S. Booth, 'Review of PREPA Technical Requirements for Interconnecting Wind and Solar Generation', NREL/TP–5D00-57089 1260328, Nov. 2013, https://doi.org/10.2172/1260328.
[33] S. Das, P.N. Suganthan, Differential evolution: a survey of the state-of-the-art, IEEE Trans. Evol. Comput. 15 (1) (Feb. 2011) 4–31, https://doi.org/10.1109/TEVC.2010.2059031.
[34] 'Renewable power generation costs in 2021', 2021.
[35] R. Wiser *et al.*, 'Land-based Wind Market Report: 2022 Edition'.
[36] Lithium-ion Battery Pack Prices Rise for First Time to an Average of $151/kWh, BloombergNEF. Accessed: Jul. 04 [Online]. Available: https://about.bnef.com/blog/lithium-ion-battery-pack-prices-rise-for-first-time-to-an-average-of-151-kwh/, 2023.
[37] N.J. Abbas, D.S. Zalkind, L. Pao, A. Wright, A reference open-source controller for fixed and floating offshore wind turbines, Wind Energy Sci. 7 (1) (Jan. 2022) 53–73, https://doi.org/10.5194/wes-7-53-2022.